Journal of Volcanology and Geothermal Research 445 (2024) 107960

Contents lists available at ScienceDirect

Journal of Volcanology and Geothermal Research

journal homepage: www.journals.elsevier.com/journal-of-volcanology-and-geothermal-research

Lithostratigraphy of the ignimbrite-dominated Miocene Bükk Foreland Volcanic Area (Central Europe)

Mátyás Hencz [a,b,c,*], Tamás Biró [a], Károly Németh [b,c,d,e], Alexandru Szakács [f], Maxim Portnyagin [g], Zoltán Cseri [a], Zoltán Pécskay [h], Csaba Szabó [b,c,i], Samuel Müller [j,1], Dávid Karátson [a]

[a] ELTE Eötvös Loránd University, Institute of Geography and Earth Sciences, Department of Physical Geography, Budapest, Hungary
[b] HUN-REN Institute of Earth Physics and Space Science, Hungarian Research Network, Sopron, Hungary
[c] MTA EPSS FluidsByDepth Lendület Research Group, HUN-REN Institute of Earth Physics and Space Science, Sopron, Hungary
[d] School of Agriculture and Environment, Massey University, Palmerston North, New Zealand
[e] National Program for Earthquakes and Volcanoes, Geohazard Research Center, Saudi Geological Survey, Jeddah, Saudi Arabia
[f] Department of Endogenous Processes, Institute of Geodynamics, Romanian Academy, Bucharest, Romania
[g] GEOMAR Helmholtz Centre for Ocean Research, Kiel, Germany
[h] Institute of Nuclear Research (ATOMKI), Isotope Climatology and Environmental Research Centre (ICER), K–Ar Group, Hungarian Research Network, Debrecen, Hungary
[i] Lithosphere Fluid Research Lab (LRG), Institute of Geography and Earth Sciences, Eötvös Loránd University, Budapest, Hungary
[j] Institute for Earth Sciences, Christian-Albrecht University of Kiel, Kiel, Germany

ARTICLE INFO

Keywords:
Correlation
Volcanic geology
Glass geochemistry
Ignimbrite
Lithostratigraphy
Phreatomagmatism
Reworked pyroclasts
Stratigraphy

ABSTRACT

This study documents the volcanic evolution of the Miocene silicic Bükk Foreland Volcanic Area (BFVA), Northern Hungary (Central Europe) at an event-scale. The BFVA is a deeply eroded and dissected volcanic field dominated by multiple, several 10-m thick, valley-filling silicic ignimbrite units, which are chemically and texturally very similar to each other. Hence, establishing lateral correlation is a real challenge due to the sporadic and small-scale outcrops and lack of stratotypes. Detailed field observations allowed us to identify eleven lithological members including fourteen eruption events and establish a nearly complete lithostratigraphic correlation between fifteen outcrops across the BFVA. Primary pyroclastic material of each member was sampled, and volcanic glass was analyzed for major and trace element composition. The geochemical results confirm the field-based classification of the members and enable the correlation of distinct outcrops. The major and trace element composition of the glassy pyroclasts of each member of the BFVA served as basis to create a field-wide chemical reference database for regional correlational studies. Here, a new lithostratigraphic classification scheme consisting of one formation and eleven members is presented, which reflects the challenges unraveling the stratigraphy of ancient volcanic terrains. The field-based event-scale lithostratigraphy of the BFVA suggests a wet, partly sea-covered depositional environment in the close vicinity of the eruption centers providing favorable conditions to 'fuel' silicic explosive phreatomagmatism. On the contrary, paleosol horizons formed after almost each major eruption event or sequence suggests an overall near-coast terrestrial environment for the BFVA, where the emplacement of the pyroclastic material occurred.

1. Introduction

In ancient volcanic areas correlating outcrop-scale pyroclastic deposits, and establishing a comprehensive lithostratigraphic framework is a real challenge because:

- outcrops suitable for establishing firm genetical interpretations are rare (Martí et al., 2018; Németh and Palmer, 2019),
- extensive weathering can significantly overprint primary sedimentary structures (Németh and Palmer, 2019),

* Corresponding author at: ELTE Eötvös Loránd University, Institute of Geography and Earth Sciences, Department of Physical Geography, Budapest, Hungary.
E-mail address: hencz.matyas@epss.hun-ren.hu (M. Hencz).
[1] Present address: Material Testing Institute, University of Stuttgart, Stuttgart, Germany.

https://doi.org/10.1016/j.jvolgeores.2023.107960
Received 11 July 2023; Received in revised form 10 October 2023; Accepted 7 November 2023
Available online 11 November 2023

- any tectonic movements may affect the original setting, in the case presented here they fragmented, uplifted or downfaulted the area,
- the scattered occurrence of the outcrops makes it difficult to recognize lateral or vertical facies changes.

Thus, a workflow and classification strategy are needed that is generally applicable to most ancient volcanic areas of the world and is consistently lithostratigraphy-based and process-oriented.

Large-scale silicic volcanism occurred in the Carpathian-Pannonian region (Central Europe) during the Miocene (Márton and Pécskay, 1998; Lukács et al., 2018). The pyroclastic deposits of this explosive volcanic flare-up crop out most continuously in the Bükk Foreland Volcanic Area (BFVA hereafter; Figs. 1, 2) but can be traced across the whole basin, found in boreholes, and in scattered and isolated occurrences on the surface as well. Occasional tephra deposits are also reported outside the Pannonian basin, however their stratigraphic correlation and link to volcanic sources are under debate (Lukács et al., 2018; Rybár et al., 2019; Brlek et al., 2023). In the BFVA the thick ignimbrites were most likely confined to broad, deep valleys or basins, hence, regional correlation (e.g., based on topographic elevation levels) will always have some uncertainty (cf. Lebti et al., 2006; Best et al., 2009).

In ancient volcanic areas, volcano-stratigraphic reconstruction is challenging due to significant weathering, vegetation cover and tectonic shifting. Moreover, recognizing pauses in the volcanism, represented by paleosols or erosional paleosurfaces, is also difficult (Németh and Palmer, 2019). The concept and terminological background of our field-focused study is based on previous works (cf. Lucchi, 2013; Martí et al., 2018; Németh and Palmer, 2019). Recognition of major unconformities makes it easier to define a volcanic lithostratigraphic unit as an unconformity-bounded stratigraphic unit (UBSU; Lucchi, 2013). However, in many cases more than one eruption center can produce pyroclastic deposits accumulating in areas located in between volcanic centers, even without distinct erosional surfaces separating them (cf. Lucchi, 2013). This is a real problem in volcanic areas characterized by eruptions from adjacent calderas with roughly coeval or partially overlapping activity (e.g., Taupo Volcanic Zone, New Zealand; Wilson, 1993) as such volcanic sources can produce volumetrically significant amounts of deposits covering extensive regions. Furthermore, besides major first-order lithostratigraphic units, minor or moderate UBSUs may often occur, not necessarily representing a significant time gap between eruptions (Martí et al., 2018), or could only represent changing eruptive style, intensity, or nature of the volcanism (Németh and Palmer, 2019; Báez et al., 2020). Unfortunately, such second- or third-order unconformities are sometimes not easily recognizable (Martí et al., 2018).

Another problem is related to the classification of volcanic deposits affected by reworking processes. Reworked volcanic material, such as deposits from gravity flows (e.g., in fluvial systems) or suspension (e.g., in aeolian and lacustrine systems), are even more difficult to link to primary volcanic processes. Chemically such deposits can be identical to their source pyroclastic deposit, thus reworked tephras cannot be classified as different eruption units despite their distinct lithological features (cf. Németh and Palmer, 2019). The eruption units of the BFVA are sparsely mapped outside its area, thus investigation of lateral facies changes is restricted to a ca. 40 × 10 km area. This makes it difficult to obtain a stratigraphic classification based on lateral facies changes (cf. Martí et al., 2018; Németh and Palmer, 2019).

In the BFVA the most recently published stratigraphic classification distinguishes ‘eruptive units’ (Lukács et al., 2018, 2022) based exclusively on zircon U-Pb dating and zircon trace element geochemistry (Table 1). As these authors mentioned, the succession of an ‘eruption phase’, within which an ‘eruptive unit’ is emplaced, may contain deposits from several eruption events that occurred within a short period of time (Lukács et al., 2018). This might be a problematic approach because “short” means thousands to hundreds of thousands of years from the perspective of the Miocene, which is potentially within the time

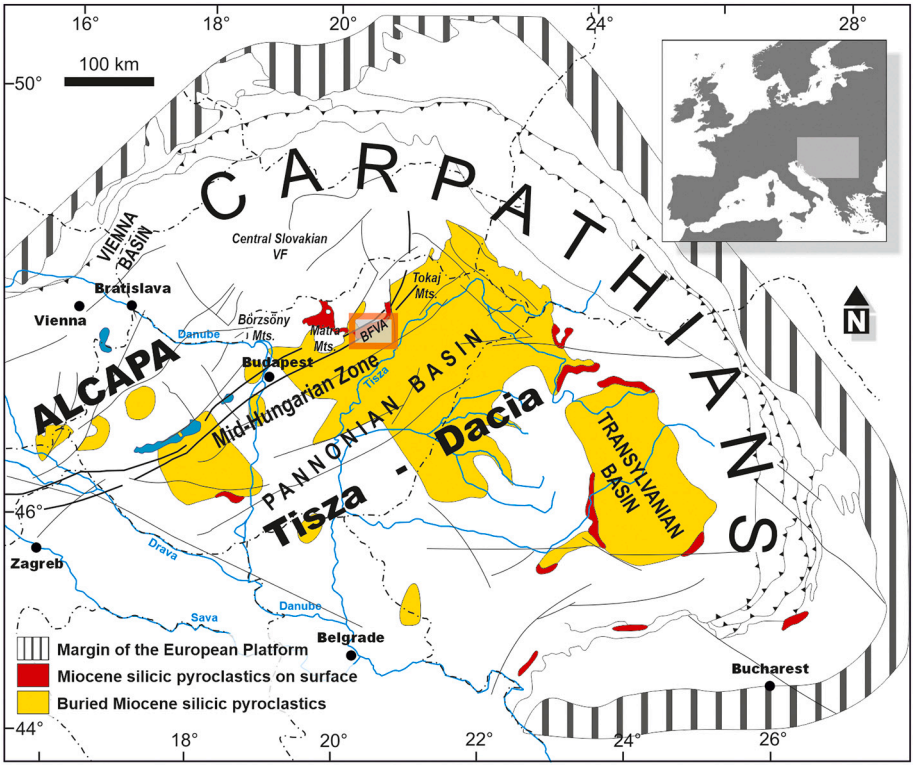

Fig. 1. Distribution of Miocene silicic pyroclastic rocks within the Carpathian-Pannonian region (Central Europe). The map was modified after Pécskay et al. (2006), Szakács et al. (2018), and Hencz et al. (2021a). Bükk Foreland Volcanic Area (Fig. 2) is indicated by rectangle with red outline. Buried pyroclastics are penetrated by drillings. (For interpretation of the references to colour in this figure legend, the reader is referred to the web version of this article.)

Table 1
Review of the stratigraphic units of the BFVA proposed in previous publications compared to this study.

Old lithostratigraphic complexes based on field observations and paleomagnetism (Szakács et al., 1998)	Old geologic formations (Gyalog and Budai, 2004)	Old chronostratigraphic units based on zircon U—Pb dating (Lukács et al., 2018)	Formal lithostratigraphic units (Lukács et al., 2022)	New members based on lithostratigraphy and volcanic glass geochemistry (this study)
UTC - Upper Tuff Complex	Galgavölgyi Rhyolite Tuff Formation	Harsány ignimbrite unit	Harsány Rhyolite Lapilli Tuff Formation	Harsány Member
	Tar Dacite Tuff Formation	Tibolddaróc unit	Tar Dacite Lapilli Tuff Formation	Tibolddaróc Member
		Demjén ignimbrite unit		Jató Member
MTC - Middle Tuff Complex		Bogács unit	Bogács Dacite Lapilli Tuff Formation	Bogács Member
ULTC - Upper Lower Tuff Complex	–	–	–	Kács Member
	–	Mangó ignimbrite unit	–	Cserépfalu Member
	Gyulakeszi Rhyolite Tuff Formation		Tihamér Rhyolite Lapilli Tuff Formation	Kisgyőr Member
		–		Tufakőbánya Member
–		–		Ostoros Member
LLTC - Lower Lower Tuff Complex		Eger ignimbrite unit		Eger Member
–	–	Csv-2 unit		Wind Member

scale of recurrent moderate volume silicic explosive events known worldwide, such as those along the Taupo Volcanic Zone in New Zealand with at least seven caldera-forming events accompanied with several dozens of silicic lava dome over 350 ky time span (Wilson, 1993, 2001). The distinguished 'units' of the BFVA were named mainly as 'ignimbrite units' (Lukács et al., 2018). In contrast, our aim was to identify, if possible, every single eruption in the volcanic record. Although field volcanological features of the area were not fully explored, our approach can be used to improve the existing schemes together with some advances in geochemical fingerprinting of pyroclastic rocks.

This paper documents and interprets the whole silicic volcaniclastic sequence of the BFVA including reworked pyroclastic deposits. We propose a far more detailed record of volcanic eruption events than currently considered, separated by long enough inter-eruption periods to allow the formation of prominent erosional surfaces and/or paleosols. We present and discuss a complete event-scale volcano-stratigraphic record of the BFVA based on field observations, focusing on the deposits interlayered between the thick ignimbrites. Geochemical examination of volcanic glass of the recognized eruption products (including thick ignimbrites) was carried out to point out the major and trace element fingerprints of these voluminous Miocene explosive eruptive flare-up events. The novelty of this approach over the North Pannonian basin is a combination of detailed field study of the event stratigraphy and precise geochemical data including major and trace elements in volcanic glass.

2. Geological background

The large-scale Miocene silicic magmatism was preceded by the subduction of an oceanic microplate (Vardar or Magura) under the ALCAPA (ALpine-CArpathian-PAnnonian) and Tisza-Dacia microplates (Szabó et al., 1992; Kovács and Szabó, 2008). The subducting plate carried volatiles (mainly H_2O), which re-fertilized the lithospheric mantle above (Kovács and Szabó, 2008). The eastward movement and rotation of the microplates caused lithospheric thinning in the middle part of the ALCAPA (Fig. 1; Csontos et al., 1992), followed by upwelling of the asthenosphere and partial melting (Seghedi et al., 2004). The resulting melt ascended through faults (formed during the movement of the microplates; Csontos et al., 1992) followed by early to late Miocene ignimbrite flare-up (Márton and Pécskay, 1998; Szakács et al., 1998).

The whole Miocene volcanic succession of the BFVA is volumetrically dominated by thick silicic ignimbrites (Fig. 2), a region inferred to

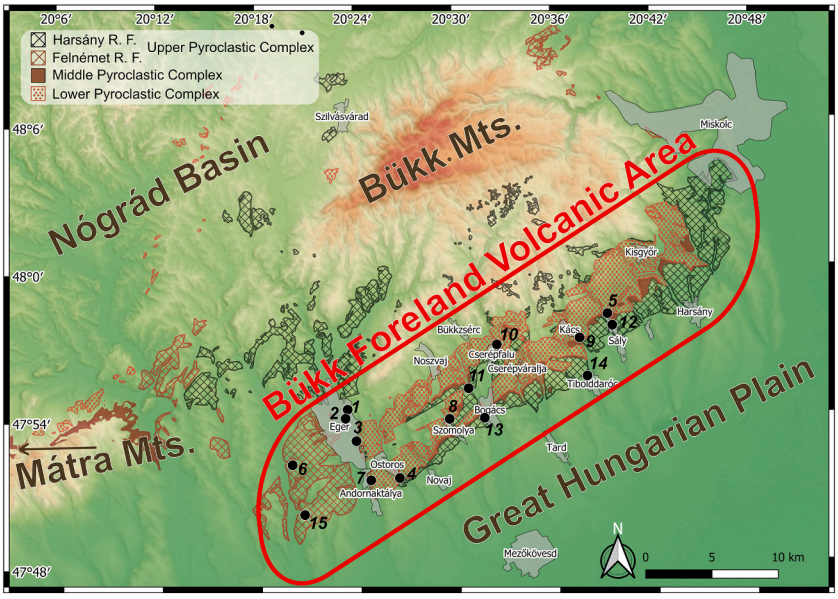

Fig. 2. Locations of the BFVA and the investigated outcrops. The locations are shown with black numbered dots; their coordinates are given in Table 2. The main pyroclastic complexes studied are shown after Szakács et al. (1998). Main settlements are shown with grey polygons. 1: Eger, Wind Brickyard, 2: Eger, Homok street, 3: Eger, Tufakőbánya, 4: Ostoros, Arany János street, 5: Sály, Latorvár, 6: Egerszalók, Skanzen, 7: Kistálya, cellars, 8: Szomolya, cellars, 9: Kács, cellars, 10: Cserépfalu, cellars, 11: Bogács, valley, 12: Sály, Dankótelep, 13: Bogács, cellars, 14: Tibolddaróc, cellars, 15: Demjén, Nagyeresztvény.

be mostly within a proximal/medial depositional area (Szakács et al., 1998; Lukács et al., 2010). Eruption centers were tentatively located in close vicinity to the BFVA based on indirect clues resulting from geological mapping, whereas their original landforms are not recognizable today (Szakács et al., 1998; Hencz et al., 2021a).

Besides the voluminous ignimbrites (several tens of meters in thickness in some cases, e.g., Karátson et al., 2022), fallout deposits of several Plinian eruptions have been recognized and mapped throughout the BFVA (Capaccioni et al., 1995; Biró et al., 2020; Hencz et al., 2021a, 2021b). Between the thick ignimbrites, paleosols (Biró et al., 2020; Hencz et al., 2021b), various *syn*-eruptive to inter-eruptive reworked and redeposited volcaniclastic layers have been recognized (Capaccioni et al., 1995; Szakács et al., 1998). Primary pyroclastic successions often display textural evidence of phreatomagmatic explosive origin (Szakács et al., 1998; Biró et al., 2020; Hencz et al., 2021b). Recently, the volcanic evolution of the BFVA was separated into eight 'eruption phases' (Table 1; Lukács et al., 2018, 2021), and later a formal lithostratigraphic classification was proposed dividing the whole pyroclastic sequence into four 'lapilli tuff formations' (Table 1; Lukács et al., 2022). Zircon U-Pb age-based geochronological methodology was used almost exclusively (with some occasional Ar-Ar ages) by the cited authors for dating the thickest and most voluminous ignimbrites.

Recent studies confirmed the complex nature of the silicic volcanism in the BFVA: in addition to magmatic explosive activity, phreatomagmatic eruptions were also common (Capaccioni et al., 1995; Szakács et al., 1998; Biró et al., 2020). The findings imply that eruption centers were located in a wet lowland setting, likely as a chain of calderas (Biró et al., 2020, 2022; Karátson et al., 2022).

The magmatic system of the BFVA can be characterized as a multi-level magmatic reservoir (Póka et al., 1998; Harangi et al., 2005; Lukács et al., 2005, 2018). Volcanism may have been fed by magmatic bodies stalled in the crust and in the vicinity of the mantle-crust boundary (Lukács et al., 2005, 2009; Seghedi et al., 2005; Czuppon et al., 2012). Crustal anatexis was invoked previously to explain the formation of silicic melts of the BFVA (Póka et al., 1998). Later, the origin of the erupted melts was explained by a complex process involving partial melting of the mantle, extensive magma fractionation, and mixing with crustal melts (Kovács and Szabó, 2008). Recent studies imply that the upper part of the magmatic system was located in the upper crust, at 4–7 km depths (Hencz et al., 2021c). Geochemical studies of the pyroclastic deposits resulted in the identification of slight differences between the thickest ignimbrite units (Póka et al., 1998; Harangi et al., 2005; Lukács et al., 2018, 2021), or chemical variations in a specified ignimbrite unit (Czuppon et al., 2012). This study makes a step forward using new state-of-art geochemical data to establish a proper chemostratigraphy and link it to lithostratigraphy.

3. Methodology

3.1. Protocol of lithostratigraphic classification

In this study we use the definitions of stratigraphic *unit* and *lithology* as follows. The UBSU scheme was hybridized with the recommendations of Németh and Palmer (2019) and Martí et al. (2018), thus the lithostratigraphic division used here is based on a) to d) below:

a) The *lithology* of each volcaniclastic layer is determined in the field and using a code to indicate the main lithological features of the layer (details in Supplementary Material 1) as suggested by Branney and Kokelaar (2002).

b) *Units* are defined as a pack of successive layers with the same lithology, or different lithology (e.g., emplacement mechanism) but consisting of primary volcaniclastic deposit only, or reworked volcanic material only, never containing material of mixed origin. In this way, it is ensured that they are genetically identical and were deposited under similar conditions and via the same emplacement mechanism. As a result, when units consist of only primary volcaniclastic deposits, they contain only geochemically identical products of a single eruption. For example, a Plinian sequence containing pyroclastic fallout deposits, dilute PDC deposits and ignimbrite (e.g., Hencz et al., 2021a) is classified as one *unit* regardless of the number or repetition of layers with the same lithological classification (e.g., Biró et al., 2020), and with no unconformity (e.g., paleosol) in between the layers. Units are labelled differently in the case of each member (e.g., Wi-1, Eg-1, Eg-2, Os-1, etc.) to avoid confusion. On the contrary, the presence of a paleosol always marks a boundary between two units because it reflects interruption in the volcanic activity. Paleosols were identified based on the following properties: clayish, dark-brown, or grey, sometimes calcified root-bearing horizon with some weak paleotopography on the top (Solleiro-Rebolledo et al., 2003). The underlying soil-forming rock is a pyroclastic rock or reworked tephra, thus, volcanic fragments can often be found in the lower part of the paleosol.

c) A pyroclastic sequence is grouped within the same member alongside its reworked upper counterpart (i.e., several units build up a member, but the pyroclastics are typically deposited from the same eruption or are reworked sediments from the same eruption). A paleosol marks a boundary not only between units, but between members, too. When no paleosol developed between two units, such as between the Eger Member and Ostoros Member, we relied on variations in geochemical composition of volcanic glass to distinguish them into separate members.

d) Correlation of different outcrops was made based on results of previous works (Biró et al., 2020; Hencz et al., 2021a) and new field-observed volcanological characteristics or volcanic glass geochemical properties of the units. Only slight lateral facies variations were detected for the identified units, which can be explained by the limited areal extent of the study area (~400 km^2), and possibly due to the almost negligible paleoaltitude differences, probably a rather flat paleotopography can be inferred (i.e., scarcity of gullies, valley-ponded or ignimbrite veneer deposits, or topography-driven undulation of pyroclastic fallout deposits).

The commonly used initial nomenclature for units exposed in the BFVA was proposed in the work of Gyalog and Budai (2004) and included the following formations: Gyulakeszi Rhyolite Tuff Formation, Tar Dacite Tuff Formation, and Galgavölgyi Rhyolite Tuff Formation. Attempts to renew the classification were published recently (see Table 1; Lukács et al., 2018, 2022). In this work, we present a new classification scheme based on detailed field mapping (lithostratigraphy) verified by analysis of volcanic glass geochemistry (major and trace elements). Such a classification is consistent with the recommendations of the International Commission on Stratigraphy (https://stratigraphy.org/guide/litho) in terms of lithostratigraphy-based formation and member classification.

In this study, a particular attention has been paid to the documentation of ash aggregates and the high volume of fine ash in order to identify eruptions which incorporated significant amount of external H_2O vapor. Note that in this work, phreatomagmatism is used to depict such eruptions showing the beforementioned signs of water influence, not its ordinary content, such as a water mediated fragmentation style (White and Valentine, 2016).

3.2. Volcanic glass geochemistry

Sampling was carried out preferably from the lowermost part of the pyroclastic rocks/layers where it was possible. Fresh glass fragments from the juvenile material of pyroclastic rocks were mounted in epoxy, polished, and analyzed for major and trace elements in GEOMAR (Kiel, Germany) using electron microprobe and in the Institute of Earth Sciences at the Christian-Albrecht University of Kiel by LA-ICP-MS. Details of the analytical methods are provided in Supplementary material 2.

4. Results

Through a detailed field examination of the pyroclastic succession of the BFVA (Fig. 2), formation and member level classification could be created. The distinguished members can be grouped in one single formation, defined here as the *Bükk Foreland Formation* (the Hungarian name should be Bükkalja Formáció) because of 1) the homogeneity in dominant grain size distribution (lapilli tuff) despite the heterogeneity of the volcanic sequence as a whole, and 2) the easily identifiable base and top surfaces, i.e. prominent, first-order lithostratigraphic boundaries within the volcanic sequence (similar, for example, to the Cassia Formation in Idaho/Nevada, USA, containing several members: Knott et al., 2016). The proposed members, along with newly designated stratotypes including their geographic coordinates and radiometric ages (if available), are summarized in Table 2. Members which are newly described by physical volcanology in this study are Ostoros Member, Tufakőbánya Member, Cserépfalu Member, Kács Member. In addition to the physical volcanological revision of the remaining members, the description strongly relies on previous works referenced in the text for each member.

In this section, we present the volcanological characteristics of each lithostratigraphically defined member of the Bükk Foreland Formation, which can be described very generally as follows. It consists of pyroclastic rocks dominated mainly by lapilli originated from magma pockets, which generated explosive eruptions and produced PDCs and pyroclastic fallout events. The formation also contains a large volume of phreatomagmatic pyroclastic deposits and several reworked pyroclastics, as well as paleosols. In the next section, general description and interpretation of the proposed eleven members of the Bükk Foreland Formation is given, completed by special features of each pyroclastic unit. The location of the outcrops can be found in Fig. 2, and their coordinates in Supplementary Material 3.

4.1. Volcanic lithostratigraphy of the Bükk Foreland Formation

4.1.1. Wind member

Description: The lowest massive lapilli tuff (mLT), deposited directly onto Oligocene – lower Miocene sandstones (Eger Formation) crops out in the Wind Brickyard stratotype location (Fig. 3). The massive lapilli tuff (Wi-1) contains max. 5–10 cm sized pumice clasts, and mainly cognate lithics 2–5 cm large (Fig. 4b, c). The total thickness of the lapilli tuff is ca. 20 m. The upper part of the lapilli tuff is heavily weathered with a clayish paleosol on the top. Fresh quartz and feldspar (often sanidine) phenocrysts are common in the lapilli tuff, the biotite phenocrysts are strongly weathered.

Interpretation: This deposit (mLT) is an ignimbrite (Wi-1; Figs. 3, 4) is clearly visible at two localities (Eger, Homok street and Eger, Wind Brickyard: Karátson et al., 2022). Earlier it was known only from boreholes (Csv-2, Lukács et al., 2018). The Wind Member potentially has a large regional distribution, because recently the same ignimbrite was identified in Croatia, cropping out several hundred kilometers from the BFVA (Brlek et al., 2023). The age of the eruption is 18.057 ± 0.018 Ma based on recent sanidine Ar-Ar dating (Karátson et al., 2022), and 18.0754 ± 0.028 Ma based on CA-ID-TIMS U-Pb zircon dating (Brlek et al., 2023).

4.1.2. Eger member

Description: The ignimbrite of the Wind Member is overlain by the pyroclastic succession of one of the largest ignimbrite-forming eruption, Eger Member, the main unit being an unwelded ignimbrite described by Capaccioni et al. (1995) and Karátson et al. (2022). The basal, inter-ignimbrite transition sequence overlying the Wind Member was documented first by Karátson et al. (2022). On top of the paleosol (Fig. 4a) there is a few cm thick, fine-grained, matrix-supported tuff with plant remnants (leaves, stems; dsT). It also contains small (mm size), core-rim type accretionary lapilli (cf. Van Eaton and Wilson, 2013: layered, concentric ash aggregate, with a coarser inner part, and a very fine outer rim). Above this, with a sharp contact, a ca. 30 cm thick, clast-supported, pumice-rich lapilli tuff/lapillistone (dsLT) crops out, capped by a thick (60–80 m), massive, poorly sorted lapilli tuff (mLT), which contains large-sized pumice blocks (20 cm typically) as well as medium-sized (over 10 cm typically) volcanic and metamorphic lithics. The phenocrystal assemblage is dominated by quartz and plagioclase, but biotite is also common. On top, alternating stratified lapilli and ash, fine-grained and coarse-grained layers occur (Eg-2). The coarse-grained layers consist of similar sized pumice lapilli with subordinate ash matrix (sLpum,acc). Plan-parallel bedding is the most common, whereas undulating beds or crossbedding are rare. Commonly, lenses of pumice and subordinate lithics with slightly rounded shape occur at the lowermost part of the thicker beds (mLpum and lensL). Some beds are extremely fine-grained, and diffusely stratified. Internally some of them contain ca. 0.5 cm sized, core-rim type (Van Eaton and Wilson, 2013) accretionary lapilli. Pumice lapilli contain abundant quartz phenocrysts.

Interpretation: The fine-grained tuff (dsT) overlying the paleosol that formed on top of the ignimbrite of the Wind Member originated from a dilute, H_2O-rich turbulent, relatively cold (~150–300 °C) PDC (indicated by the presence of ash aggregates and paleomagnetic properties; Karátson et al., 2022). The following well-sorted lapilli tuff/lapillistone (dsLT) unit was deposited as a fallout pyroclastic deposit from a stable eruption column, which later destabilized, collapsed, and caused a PDC

Table 2
The new volcanic members and their stratotype localities with available age estimates. The members documented for the first time in this work are highlighted in bold.

New members	Stratotype locality	Coordinates	Age (Ma)*	Age measurement method	Age measurement reference
Wind Member	Eger, Wind Brickyard	47°53′48.6"N 20°23′57.4"E	18.2 ± 0.3	zircon U-Pb	Lukács et al., 2018
			18.057 ± 0.018	sanidine Ar-Ar	Karátson et al., 2022
			18.0754 ± 0.028	CA-ID-TIMS U-Pb zircon	Brlek et al., 2023
Eger Member	Eger, Homok street	47°53′40.9"N 20°24′03.2"E	17.5 ± 0.3	zircon U-Pb	Lukács et al., 2018
	or	47°53′09.4"N 20°23′59.1"E	17.25 ± 0.11	plagioclase Ar-Ar	Karátson et al., 2022
	Eger, Tufakőbánya, lower quarry		17.327 ± 0.023	CA-ID-TIMS U-Pb zircon	Brlek et al., 2023
Ostoros Member	Ostoros, cellars	47°51′39.2"N 20°26′18.1"E	n.d.	–	–
Tufakőbánya Member	Eger, Tufakőbánya, upper quarry	47°53′08.6"N 20°24′14.5"E	n.d.	–	–
Kisgyőr Member	Eger, Tufakőbánya, upper quarry	47°53′08.6"N 20°24′14.5"E	17.055 ± 0.024	ID-TIMS zircon U-Pb	Lukács et al., 2018
Cserépfalu Member	Cserépfalu, cellars	47°56′40.1"N 20°32′30.9"E	17.14 ± 0.12 (?)	zircon U-Pb	Lukács et al., 2018
Kács Member	Kács, cellars	47°57′04.4"N 20°37′25.5"E	n.d.	–	–
Bogács Member	Kács, cellars	47°57′04.4"N 20°37′25.5"E	16.816 ± 0.059	ID-TIMS zircon U-Pb	Lukács et al., 2018
Jató Member	Bogács, cellars	47°53′47.2"N 20°31′38.3"E	14.88 ± 0.014	ID-TIMS zircon U-Pb	Lukács et al., 2018
Tibolddaróc Member	Tibolddaróc, cellars	47°55′27.0"N 20°37′49.8"E	14.7 ± 0.2	zircon U-Pb	Lukács et al., 2018
Harsány Member	Tibolddaróc, cellars	47°55′27.0"N 20°37′49.8"E	14.358 ± 0.015	plagioclase Ar-Ar	Lukács et al., 2018

* Published age constraints are adopted to the new scheme presented in this study.

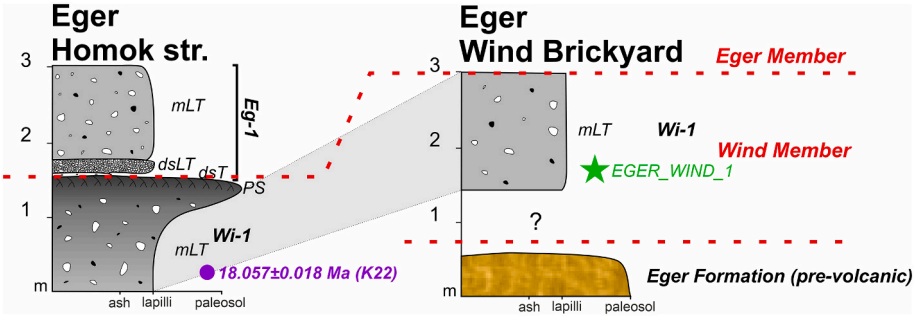

Fig. 3. Transition from the Oligocene pre-volcanic Eger Formation to the Eger Member. For lithologic abbreviations see Supplementary Material 1. Purple dot represents relative stratigraphic position of previously dated sample (K22: Karátson et al., 2022; Table 2). Labelled green stars show the stratigraphic position and name of geochemically analyzed samples. (For interpretation of the references to colour in this figure legend, the reader is referred to the web version of this article.)

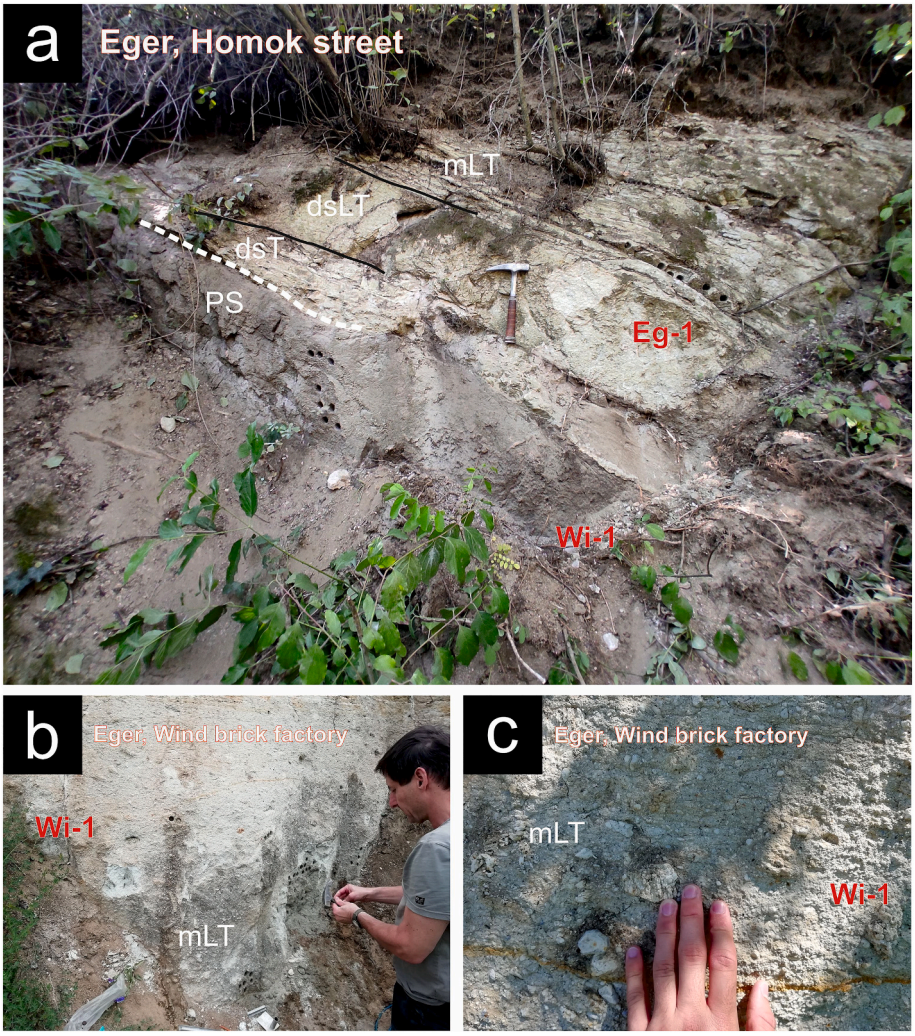

Fig. 4. Representative pictures showing the field characteristics of the Wind and Eger Members. a. Outcrop in the Homok Street in Eger, where the transition between Wi-1 and Eg-1 is revealed. b. Typical outcrop of Wind Member at the top of the Oligocene sequence of Eger Formation. c. Close-up view of Wi-1. The outcrop here is significantly weathered (see brownish iron precipitation). For lithologic abbreviations see Supplementary Material 1.

(ignimbrite). This ignimbrite, previously named "Eger Ignimbrite", is 17.25 ± 0.11 Ma old (plagioclase Ar-Ar, Karátson et al., 2022). Based on field observations, in the eastern BFVA this member is absent, thus the eruption center might be in the west/southwest of the BFVA (Karátson et al., 2022). Recently, the ignimbrite was recognized in the Kalnik region (Croatia) 300 km southwestward and correlated to the BFVA occurrences using zircon geochemistry and high precision zircon U-Pb ages (17.327 ± 0.023 Ma, Brlek et al., 2023). Occurrences over such large distances suggest a voluminous, significant explosive eruption. On top of this ignimbrite a reworked sequence is found (Eg-2), which mostly consists of components of the ignimbrite (mLT) below. The co-ignimbrite ash was most probably impacted by external water as indicated by the presence of abundant core-rim type accretionary lapilli in the reworked deposit (sLpum,acc; cf. Van Eaton and Wilson, 2013).

Reworking could take place through energetic hyper-concentrated flows, as suggested by the presence of pumice and lithics in lens (cf. Di Capua and Scasso, 2020).

4.1.3. Ostoros member

Description: This newly-defined member consists of deposits with six different lithologies (Fig. 5; Os-1 and Os-2). The lowermost deposit starts with a cross-bedded, fine-grained tuff (xsT), with diffuse transition to the upper massive, quartz-free, pumice-bearing, poorly sorted lapilli tuff (mLT) deposited with erosional contact. This lapilli tuff is inversely graded, the largest pumice clasts are found in the uppermost part. Above it, a 10 cm thick lapilli tuff crops out, which consists of mainly core-rim type accretionary lapilli, and subordinate fine ash matrix (dsLTacc; Fig. 6a). Over this, a 5–6 m thick fine-grained lapilli tuff follows (mLTpip,acc), which contains abundant, 4–5 cm large, complexly-layered (fine- and coarse-grained internal layers alternating; terminology after Van Eaton and Wilson, 2013), often deformed accretionary lapilli close to its base (Fig. 6b, c). These lapilli are present mainly concentrated in gas segregation pipes, although the matrix also contains randomly occurring, complexly layered accretionary lapilli along with abundant core-rim type accretionary lapilli. Accretionary lapilli fragments are also present. Pumice clast size is in the range of a few centimeters, whereas lithics are typically in the mm range. The deposit is dominated by a fine ash matrix. At the uppermost part of the lapilli tuff, core-rim type accretionary lapilli are grouped in fan-shaped gas segregation pipes, complexly layered accretionary lapilli are rare (Fig. 6d; Os-1). A volcanogenic sand unit crops out in high stratigraphic position (Os-2), and contains reworked material (e.g., clasts from the lower, accretionary lapilli-bearing lapilli tuff). At its lowermost part, accretionary lapilli, and 5–6 cm large, slightly rounded pumice clasts and subordinately lithics can be seen (sVSacc). On top, a brownish grey paleosol developed (PS).

Interpretation: This member differs from the Eger Member not only in its complexity, but also in the absence of quartz in the phenocryst assemblage. The member starts with a dilute, turbulent PDC deposit (xsT), followed by a more typical 'dry', magmatic ignimbrite (mLT). Without any erosional surface it is overlain by a phreatomagmatic fallout deposit (dsLTacc). The core-rim type accretionary lapilli were created from ash aggregates which fell into the water-rich co-ignimbrite ash (Van Eaton and Wilson, 2013). The abrupt change in the eruption style from purely magmatic to phreatomagmatic could be caused by caldera wall collapse allowing water invasion to the eruption center, a scenario described earlier for the Jató Member (Biró et al., 2020). Then, the eruption column collapsed, and a phreatomagmatic ignimbrite deposited (mLTpip,acc). The abundance of complexly layered accretionary lapilli as well as the fragments of accretionary lapilli suggests that the deposit originated from a moist pyroclastic density current (Van Eaton and Wilson, 2013). On top, the primary pyroclastic material shows reworking (sVSacc) by energetic, secondary processes reflecting abundant water (e.g., hyperconcentrated flows, lahars).

4.1.4. Tufakőbánya member

Description: Tufakőbánya Member is composed a ca. 1 m thick well-sorted, pumice clast-supported lapilli tuff deposited with a maximum clast diameter of 5–6 cm (dsLT; Fig. 5), described schematically by Capaccioni et al. (1995). With diffuse transition, this is overlain by a 2 m-thick stratified tuff-lapilli tuff sequence (sTacc, sLTacc; Fig. 6e). Some layers are well-sorted, others poorly sorted. The layers vary in thickness from a few centimeters to 40 cm. Fine-grained tuffs (sTacc) often contain 0.5–1 cm-sized core-rim type accretionary lapilli (Fig. 6f). The sequence continues with several beds of different lithologies (Tu-2), consisting of reworked volcanic materials (dsLpum,lit, sLlit, dsLpum). Pumice clasts show normal to inverse grading. The deposits are poorly sorted and typically quartz-free. Two very characteristic, lithic-rich, 10 cm thick, undulating marker horizons are present, making lateral correlation (sLlit) easier. Internal stratification in each layer is common. There is a

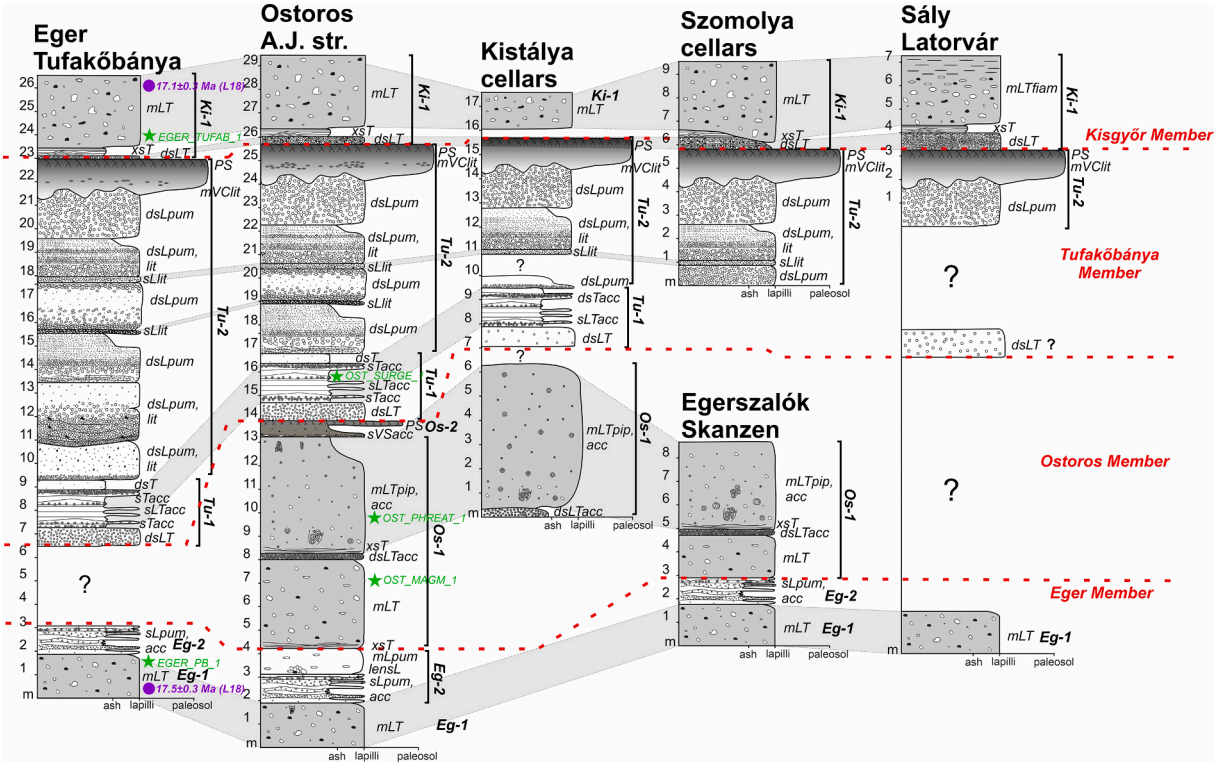

Fig. 5. Lithostratigraphic section between Eger and Kisgyőr Members for all described outcrops. For lithologic abbreviations see Supplementary Material 1. Purple dot represents relative stratigraphic position of previously dated samples (L18: Lukács et al., 2018; Table 2). Labelled green stars show the stratigraphic position and name of geochemically analyzed samples. (For interpretation of the references to colour in this figure legend, the reader is referred to the web version of this article.)

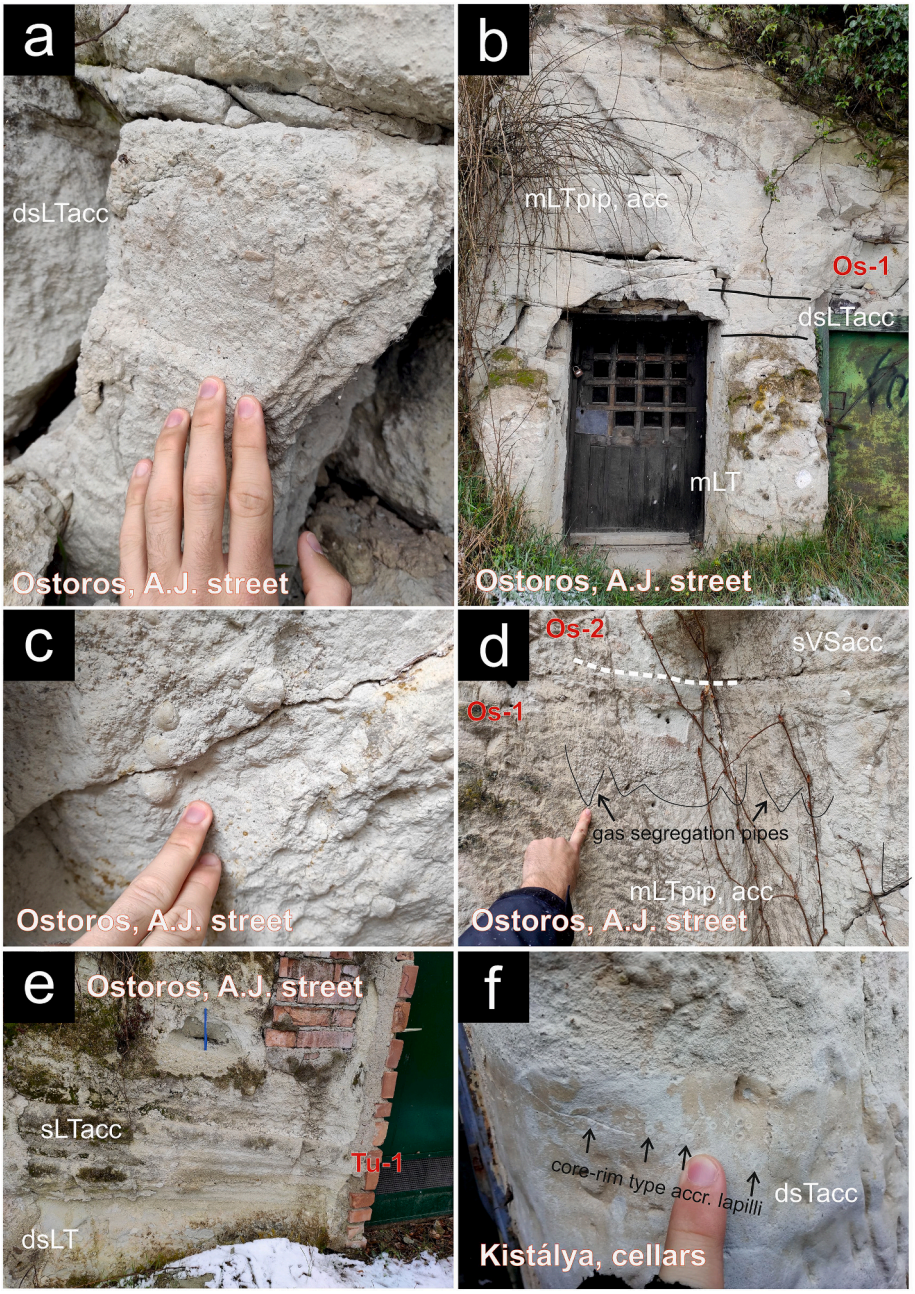

Fig. 6. Field pictures with close-ups of Ostoros and Tufakőbánya Members a. A layer containing abundant accretionary lapilli in the middle part of Os-1 of the Ostoros series. b. Field appearance of Os-1. The lower mLT also contains large pumice clasts as seen in the lower right of the image. c. Extremely large, complexly layered accretionary lapilli in the mLTpip,acc lithology pyroclastics of Os-1. d. Top of Os-1. The fan-shaped gas segregation pipes are enriched in core-rim type accretionary lapilli. e. Stratified sequence of Tu-1. f. Close-up photograph of a fine-grained layer of Tu-1. Arrows mark some small-scale, core-rim type accretionary lapilli. For abbreviations see Supplementary Material 1.

poorly sorted, diffusely bedded, brownish-grey, clayish volcanogenic sediment with rounded, dark-colored volcanic lithics deposited in lenses (mVClit). On this deposit dark brown paleosol was formed which often contains calcified roots or other plant remnants.

Interpretation: The lower part of the member probably consists of primary volcanic material. The field characteristics of the deposit suggest that it is a sequence of well-sorted pyroclastic fallout (dsLT) and fine-grained, poorly sorted, dilute PDC deposits (sTacc, sLTacc, dsT). The core-rim type accretionary lapilli occurring in the fine-grained layers suggests input of external water which caused minor phreatomagmatic fragmentation. There is no primary volcanic deposit in the upper sequence of the member; all layers have varying thickness suggesting a dynamic process, which could include fluvial processes or laharic mass flow events (cf. Lavigne et al., 2000; Segschneider et al., 2002).

4.1.5. *Kisgyőr member*

Description: From a volcanological point of view, this member was studied in detail by Hencz et al. (2021a), and earlier by Capaccioni et al. (1995) and Biró et al. (2017). The sequence starts with a well-sorted, clast-supported lapilli tuff/lapillistone (dsLT) layer with mm-sized quartz crystals and up to 15 cm large lithics and pumice (Figs. 7, 8). Thickness of layer decreases from 90 to 20 cm westward (Hencz et al., 2021a). The capping sediment is a cross-bedded fine tuff (xsT) with mm-sized pumice clasts, showing diffuse transition to the following massive lapilli tuff (mLT) with large (>20 cm) pumice and lithic clasts in an ash

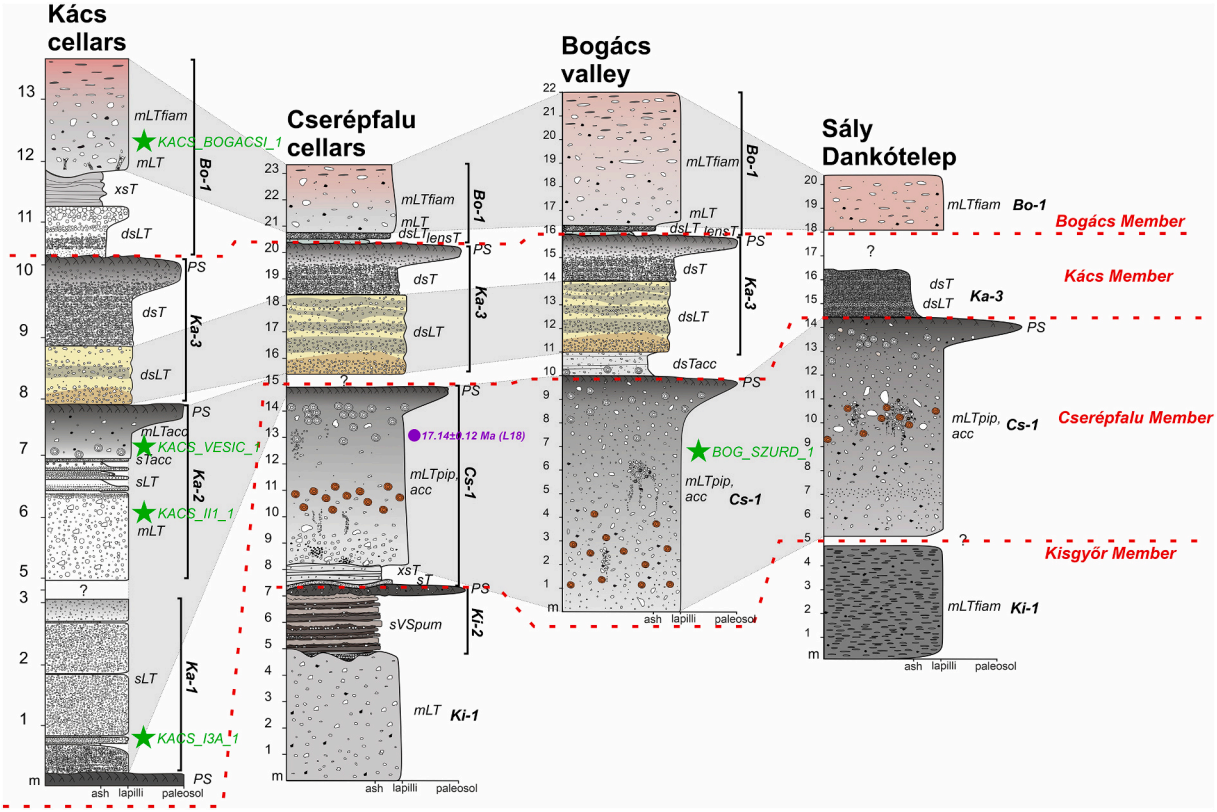

Fig. 7. Lithostratigraphic section between Kisgyőr and Bogács Members for each outcrop. Some analogue deposits are tentatively correlated. For lithologic abbreviations see Supplementary Material 1. Purple dot represents relative stratigraphic position of previously dated sample (L18: Lukács et al., 2018; Table 2). Labelled green stars show the stratigraphic position and name of geochemically analyzed samples. (For interpretation of the references to colour in this figure legend, the reader is referred to the web version of this article.)

matrix. The lapilli tuff shows fiamme-like welding characteristics (mLTfiam), more common in the eastern outcrops (e.g., at Sály – Latorvár, Fig. 2). The phenocryst population is dominated by light purple, euhedral-subhedral quartz, biotite, and plagioclase (Ki-1 in Figs. 5, 7). Covering the lapilli tuff, volcanogenic sandstone or claystone (sVSpum) crops out (Ki-2), which consist of up to 20 cm thick layers of sand or mud-sized components. Outsized pumice clasts (over 10 cm in diameter) are commonly found in this unit. In some of the layers, slightly rounded pumice clasts are segregated in lenses.

Interpretation: The member starts with a pyroclastic fallout (dsLT), followed by a deposit generated by a turbulent, dilute PDC from a destabilized eruption column (xsT). Then, due to complete column collapse, a massive ignimbrite (mLT) closes the succession reaching up to 240 m thickness (in boreholes, Lukács et al., 2010) in the east, and about 50 m in the vicinity of Eger, west from the BFVA. The eruption center was likely located to the east of the BFVA as inferred from thickness and granulometric characteristics of the fallout layer (Hencz et al., 2021a), confirming the hypothesis of Lukács et al., (2010). The layered volcanogenic clayish layers deposited on top of the ignimbrite (sVSpum) can be a result of resedimentation by lahar(s) (Lavigne et al., 2000; Segschneider et al., 2002), like it is observed on top of the Tufakőbánya Member. The age of this member is 17.055 ± 0.024 Ma (zircon U-Pb, Lukács et al., 2018).

4.1.6. *Cserépfalu member*

Description: Never identified before, this member consists of a stratified tuff (sT) followed by a cross-stratified tuff (xsT), and finally a 7 to 10 m thick, massive, relatively fine-grained lapilli tuff (mLTpip,acc) with gas segregation pipes and abundant, large (>3 cm), complexly layered and core-rim type accretionary lapilli (Figs. 7, 8a, b, c; Cs-1). The massive lapilli tuff contains pumice clasts (5 cm on average), and subordinate lithic clasts (in the mm range). Quartz, biotite, and feldspar phenocrysts rarely occur. The outer crust of the complexly layered accretionary lapilli is heavily weathered and have an orange-brown colour (Fig. 8b). A paleosol was found at the top of the layer.

Interpretation: The member on top of the underlying paleosol starts with a pyroclastic fallout (sT), then a deposit from a dilute PDC follows (xsT), and the succession ends with a several meters thick accretionary lapilli-bearing phreatomagmatic ignimbrite (mLTpip,acc). The accretionary lapilli are complexly layered suggesting a phreatomagmatic origin for the ignimbrite. Thus, the member represents a typical Plinian, or rather Phreatoplinian (sensu lato) sequence (fallout – dilute PDC – PDC deposit). The age of this member (17.14 ± 0.12 Ma based on zircon U-Pb dating, Lukács et al., 2018) is very close to Kisgyőr Member (17.055 ± 0.024 Ma, zircon U-Pb, Lukács et al., 2018), thus, in recent works (Lukács et al., 2018, 2022) these outcrops was classified as identical occurrence to the outcrops of Kisgyőr Member.

4.1.7. *Kács member*

Description: The Kács Member (containing units Ka-1, Ka-2, and Ka-3) was described by Hencz et al. (2021b) based on granulometric and paleomagnetic measurements. Here, the Kács Member is presented as a single member, despite some geochemical properties (see below) suggest that it is composed of 3 different units with slightly different compositions. On this basis, there are three units but because of there is only one single outcrop of Ka-1 and Ka-2 in the whole BFVA, the three units were grouped together into one member (Fig. 7). The lower part of the member consists of well-sorted, clast-supported lapilli tuff horizons (Ka-1). Fine-grained tuff – lapilli tuff layers are present between coarse-grained lapilli tuff layers (sLT). The pumice clasts are 3–4 cm in diameter in the coarser layers, and 4–5 mm large in the finer ones. The layers consist of cm-sized pumice lapilli and subordinate lithic clasts. Crystals

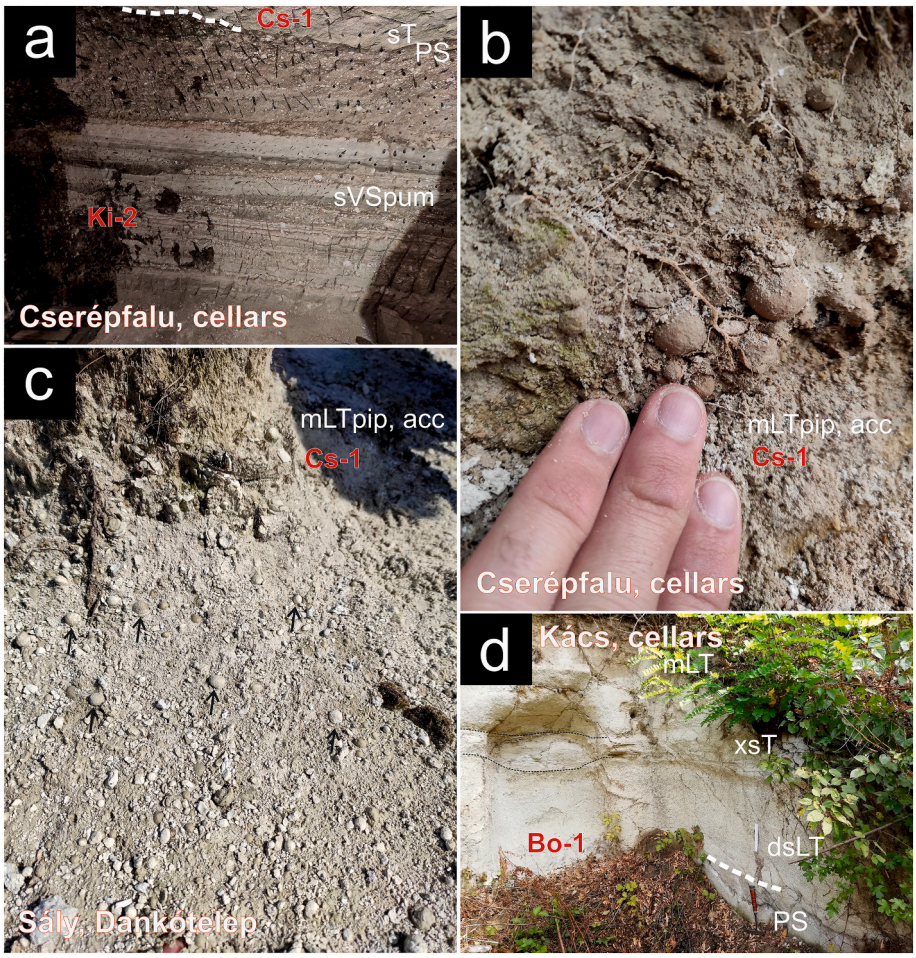

Fig. 8. Field pictures and details of Cserépfalu, Kács and Bogács Members a. Densely stratified, volcanogenic sandstone sequence of Ki-2 (Fig. 7). In several places, larger, white-colored pumice clasts are visible. b. In Cs-1, large, complexly layered accretionary lapilli with a yellowish-brown, fine-grained outer crust. c. Abundant presence of accretionary lapilli in Cs-1. Often these are enriched in gas segregation structures. d. Well-sorted lapilli tuff (dsLT), cross-laminated tuff of undulating thickness (xsT), and massive lapilli tuff (mLT), which shows upward gradual welding at the base of Bo-1 (Fig. 7). For abbreviations see Supplementary Material 1. (For interpretation of the references to colour in this figure legend, the reader is referred to the web version of this article.)

and crystal fragments are rare, and plagioclase is the most common mineral. It was deposited on top of a well-developed paleosol, but the deposit below the paleosol is unknown. Thus, the underlying pre-soil deposit cannot be determined. The unit above this (Ka-2) starts with a poorly sorted massive lapilli tuff (mLT), followed by coarse-grained tuff and lapilli tuff layers (sLT). On the top of the unit, stratified accretionary lapilli-bearing tuff (sTacc), and a poorly sorted, accretionary lapilli-bearing, highly weathered, massive lapilli tuff occur (mLTacc). On its top another paleosol (PS) horizon formed which in turn is followed by a well-sorted, clast-supported, strongly weathered lapilli tuff (dsLT; Ka-3). It contains quartz phenocrysts. Diffuse internal stratification is present. The uppermost part of the unit consists of diffusely stratified normal-graded coarse tuff (dsT), whose grain size decreases upwards. On the top, well-developed paleosol (PS) was formed (Fig. 8d).

Interpretation: The sequence's lowest part represents layers originating from pyroclastic fallout (sLT), followed by a hiatus in the eruptive activity. The coarse-grained, poorly sorted characteristics of the lapilli tuff deposited next suggests a PDC origin (mLT). Then, a repeatedly, but partly collapsing eruption column caused dilute, turbulent PDCs (sLT, sTacc), whereas the presence of accretionary lapilli suggests the intervening external water, and a resulted moist eruption column. On top, a paleosol formed, then from another eruption a stable eruption column produced a diffusely stratified pyroclastic-fall sequence (dsLT, dsT), which was followed again by a paleosol. There are stratigraphic profiles without any hiatus between the Cserépfalu and Bogács Members (Fig. 7). If other outcrops also represent this part of the stratigraphic log, the Kács Member can be identified as a meter or a few meters thick fine-grained tuff containing accretionary lapilli. We assume that this sequence is eroded elsewhere, thus only its proximal part is preserved in the geological record. There were not any age constraints published recently.

4.1.8. *Bogács member*

Description: The Bogács Member starts with a mantle-bedded, diffusely stratified, clast-supported lapilli tuff (dsLT) with up to 5 cm large pumice and 1 cm large lithic clasts (Figs. 7, 8d; Bo-1). The thickness of the layer is about 20 cm in the case of western outcrops (Cserépfalu – cellars, Bogács – valley), and reaches about 80 cm at Kács – cellars site, its easternmost outcrop. A stratified, poorly sorted tuff with cross-bedding and undulating layer thickness (xsT) follows with a sharp lower contact. This deposit has a diffuse contact to the capping, massive, pumice-bearing lapilli tuff (mLT), which contains subordinate quartz phenocrysts, whereas biotite, amphibole and plagioclase are the typical mineral assemblage. Maximum pumice clast size is 20 cm, and the lithics are up to 5 cm in diameter. The lapilli tuff shows welding characteristics upward, i.e., a few meters from the contact, where the bottom of the unit is visible: the pumice clasts are flattened, often showing fiamme structures (mLTfiam). The total thickness of this lapilli tuff horizon is greater in the east (up to 100 m in boreholes): at the Cserépfalu – cellars site, for example, its thickness is about 15 m. In the upper part of this lapilli tuff,

dark grey-colored scoria clasts also occur. At the top (Bo-2) a well-sorted, fine-grained fine tuff with sharp contact crops out. It contains abundant, large (max. 3 cm in diameter) accretionary lapilli (dsLTacc). Quartz is subordinate, biotite, amphibole and feldspar are abundant. It is highly weathered, clayish, unlikely to be interpreted as an entirely primary volcanic deposit.

Interpretation: The member represents again a complete Plinian eruption sequence (dsLT-xsT-mLT), where a high-grade ignimbrite (mLTfiam) closes the eruption. The welding of the ignimbrite starts a few meters above the lower boundary of the ignimbrite forming fiamme structures. Towards the top of the ignimbrite most of the lithics are juvenile grey-colored mafic scoria clasts, whose presence should be considered as evidence of magma mingling as described earlier (Szakács et al., 1998; Czuppon et al., 2012). Based on the thickness variation of the basal Plinian fallout deposit (dsLT; 20 cm in the west, 80 cm in the east) an eruption center east-southeast of the BFVA can be tentatively inferred, which was suggested at a nearby location based on AMS data of the welded ignimbrite (Szakács et al., 1998). The top of the ignimbrite is rarely preserved. In most cases, the post-volcanic erosion significantly impacted this part of the ignimbrite: the deposit (dsLTacc, dsTacc) sitting on top is highly weathered, clayish, however, accretionary lapilli, suggestive of magma-water interaction can be observed (Capaccioni et al., 1995). The zircon U-Pb age of the welded ignimbrite (i.e., 16.816 ± 0.059 Ma) and the capping phreatomagmatic (probably partly redeposited) sub-unit (16.7 ± 0.3 Ma: Lukács et al., 2015) are analytically indistinguishable, therefore they can be considered as belonging to the same member, the Bogács Member. The closing unit can be interpreted as a co-ignimbrite phreatomagmatic ash, or as a final-stage phreatomagmatic phase of the volcanism of the Bogács Member.

4.1.9. Jató member

Description: Biró et al. (2020) introduced this unit as a newly defined member. Their results are summarized here (Fig. 9). The lower part consists of coarse tuff layers and 2–20 cm thick lapilli tuff layers with a laterally constant thickness (sLT). These layers are well-sorted and contain mainly pumice fragments, sparse lithics and phenocrysts (biotite, feldspar, green amphibole, but quartz is absent). In the upper part, the layers are fine-grained, showing undulating thickness (Fig. 10a, b). The basal part of the layers is coarser-grained, whereas the upper part is finer-grained, showing normal gradation. In the upper part accretionary lapilli are abundant (sTacc; Fig. 10c, d). The uppermost deposit is a massive, 3–4 m thick lapilli tuff with pumice clasts up to 2 cm in diameter. This lapilli tuff contains gas segregation pipes in the lower part, and accretionary lapilli at the base (mLTpip,acc; Fig. 10b). The uppermost 1–2 m is highly weathered, brown in colour. On top is a brown paleosol (PS). At Demjén – Nagyeresztvény locality, the identical (Lukács et al., 2015, 2018) massive, thick, but relatively fine-grained lapilli tuff shows characteristics of welding (e.g., fiamme structures) in its middle part (mLTfiam).

Interpretation: The lower ca. 2 m thick part of this member originated from a stable Plinian eruption column and deposited as pyroclastic fallout layers (sLT). Then, the dominant fragmentation type changed abruptly, and phreatomagmatism took over: dilute PDCs spread across the terrain from a gradually collapsing eruption column due to the influence of incoming external water (sTacc). Finally, the eruption column collapsed, and a fine-grained, partly phreatomagmatic ignimbrite deposited (mLTacc, mLTpip,acc). As Biró et al. (2020) suggested, the eruption type was sensu lato Phreatoplinian. Based on zircon U-Pb dating (14.880 ± 0.014 Ma, Lukács et al., 2018), the ignimbrite of the Jató member is similar in age to the slightly welded ignimbrite (mLTfiam) of Demjén – Nagyeresztvény.

4.1.10. Tibolddaróc member

Description: The Tibolddaróc Member is an about 3 m thick

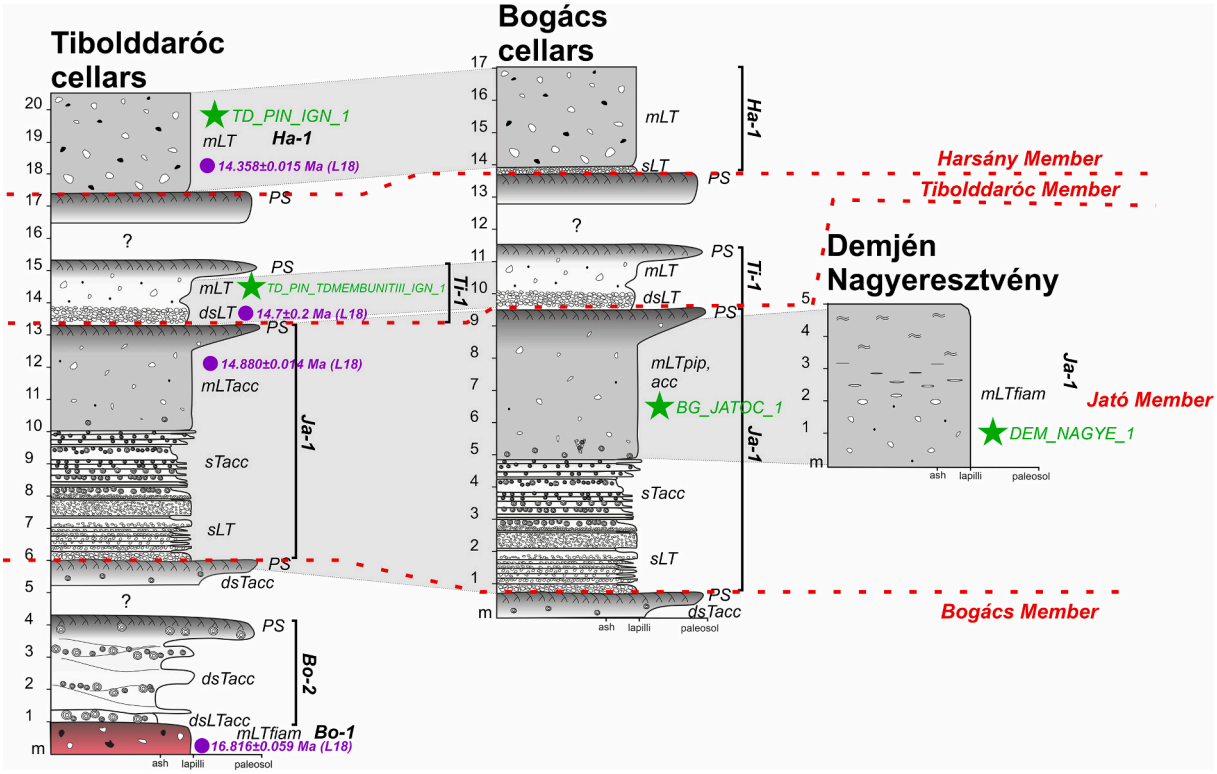

Fig. 9. Lithostratigraphic section between Bogács and Harsány Members for all described outcrops. Some analogue deposits are correlated. For lithologic abbreviations see Supplementary Material 1. Purple dot represents relative stratigraphic position of previously dated samples (L18: Lukács et al., 2018; Table 2). Labelled green stars show the stratigraphic position and name of geochemically analyzed samples. (For interpretation of the references to colour in this figure legend, the reader is referred to the web version of this article.)

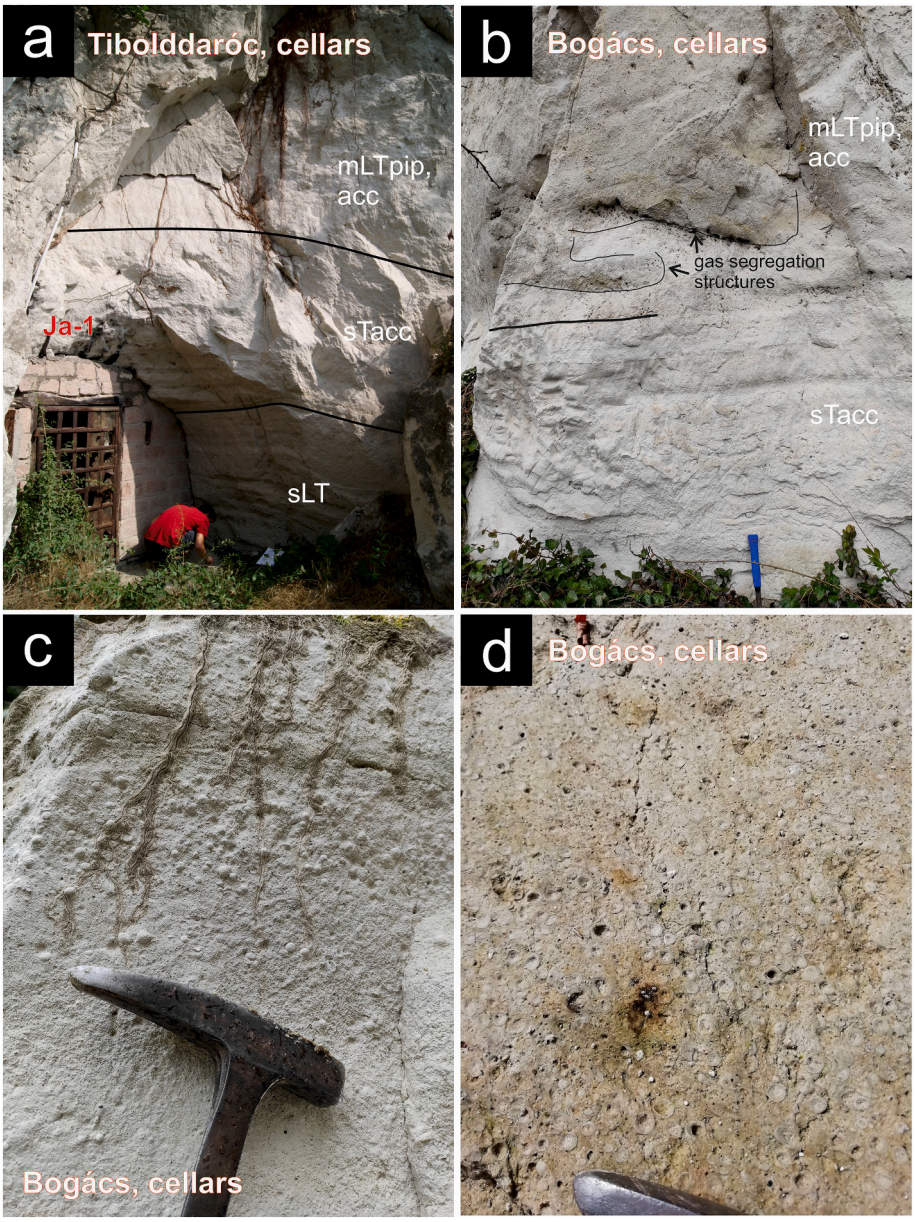

Fig. 10. Field pictures and details of deposits of the Jató Member: a. main lithological subunits of Ja-1. b. Transition of the massive lapilli tuff and stratified tuff at the top of Ja-1. Several coarse-grained zones (gas segregation pipes) are present at the base of the massive lapilli tuff. c. An sTacc lithology layer of Ja-1, where the core-rim type accretionary lapilli is reverse graded within the layer. d. Horizontal section of an sTacc lithology layer of Ja-1. The core-rim type of accretionary lapilli appears in masses. Amorphous or broken accretionary lapilli are also frequently seen. For abbreviations see Supplementary Material 1.

succession, which consists of fine-grained and coarse-grained lapilli tuff layers (Fig. 9; Ti-1). The lower part reveals a well-sorted sequence (dsLT), whereas the upper part poorly sorted lapilli tuffs (mLT). Besides biotite and feldspar, quartz is subordinate. The whole member is highly weathered, especially at its lower part. On the top, following a stratigraphic hiatus (ca. 1 m does not crop out), a well-developed paleosol (PS) was formed.

Interpretation: This member may be distinguished from the older Jató and the younger Harsány Members due to the age difference according to the published, though overlapping zircon U-Pb ages (Demjén/Jató: 14.88 ± 0.04 Ma, Tibolddaróc: 14.7 ± 0.2 Ma, Harsány: 14.3 ± 0.2 Ma; Lukács et al., 2018). Based on field characteristics, the member originated from a stable Plinian eruption column, and deposited as a pyroclastic fallout sequence (mLT). The poorly sorted upper part is an ignimbrite (mLT) that deposited from a collapsing Plinian eruption column.

4.1.11. *Harsány member*

Description: The Harsany Member lies on top of the abovementioned paleosol and is a 20 cm thick, well-sorted, clast-supported lapilli tuff or lapilli stone deposit (sLT), which is present only at Bogács village due to the erosional effect of the overlying massive, quartz-rich, large (>20 cm) pumice-bearing lapilli tuff (mLT; Fig. 9; Ha-1) of the Tibolddaróc member. The total thickness of this member cannot be inferred because the top level is eroded everywhere.

Interpretation: The Harsány Member represents a Plinian sequence starting with a Plinian fallout deposit (sLT) followed by an ignimbrite (mLT). This member is observed only in the easternmost part of the BFVA. Based on the solely eastern occurrences, an eastern eruption center might be inferred. However, a distal fallout attributed to this member was recognized recently in the westernmost part of the Mátra Mountains (Lukács et al., 2021). The zircon U-Pb age of this member is 14.3 ± 0.2 Ma (Lukács et al., 2018).

4.2. Major and trace element volcanic glass chemistry

Pyroclastic samples for geochemical study were collected from the lower part of the pyroclastic layers wherever it was possible. Thus, the results do not represent the whole sequence (i.e., geochemically heterogeneous eruptions may have occurred, see Szakács et al., 1998, Czuppon et al., 2012, Brlek et al., 2023), but they give a general picture about the geochemical properties of the volcanic glass of the analyzed unit. Variations of FeO vs. TiO_2, Nb vs. Y, Nb/Y vs. Ta/Yb, and Th vs. Zr/Sr ratio were used for discrimination of the studied members (Fig. 11a, b, c, d). Relative chronological position versus major or trace element compositions and ratios were plotted next to the stratigraphic column to illustrate the variations of the geochemical characteristics over time (Fig. 12).

All pyroclastic deposits are high-K (>4 wt% K_2O), high-SiO_2 rhyolites with nearly similar (75–78 wt%) SiO_2 composition. Most samples

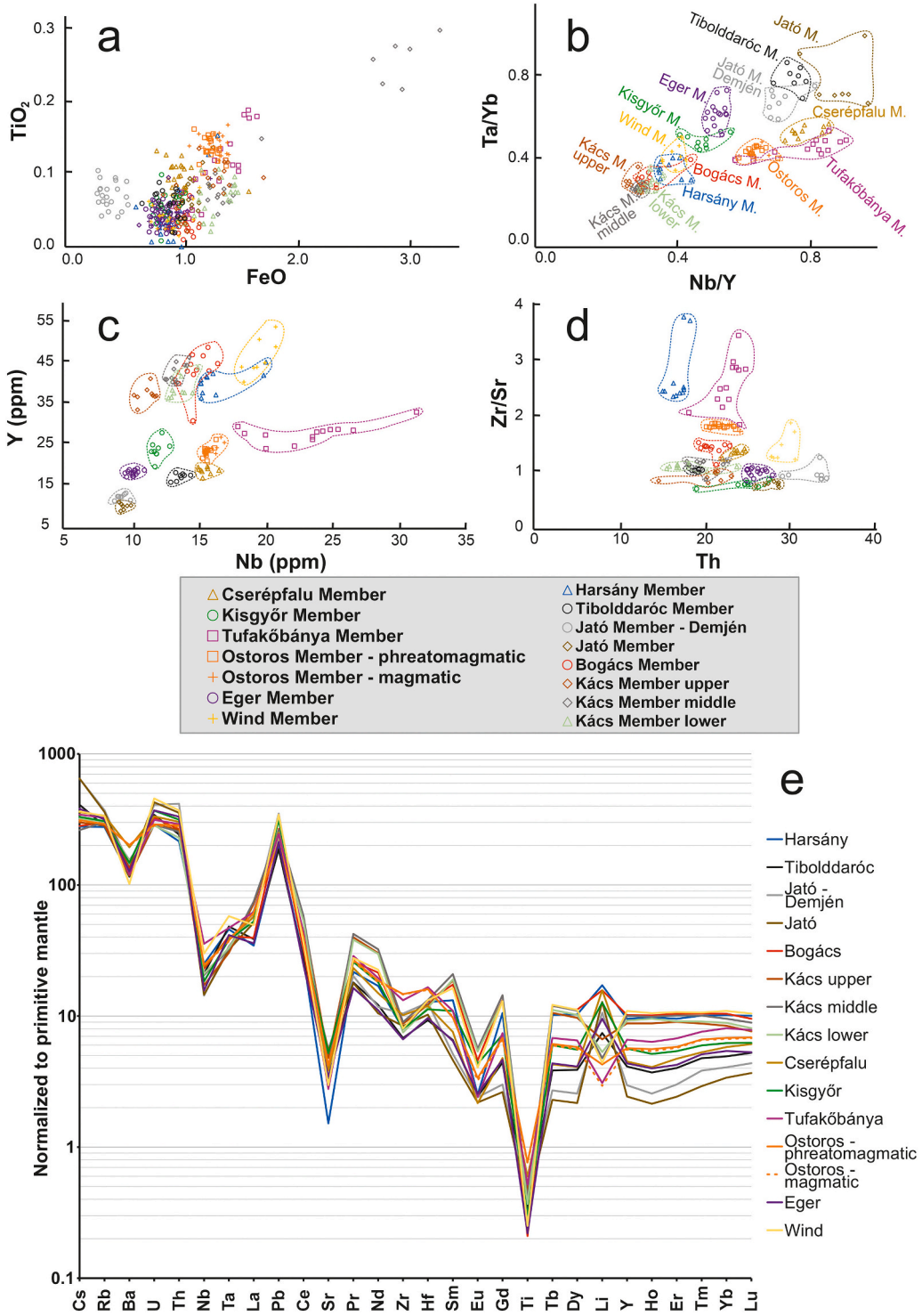

Fig. 11. Major and trace element composition of studied samples: a: FeO vs. TiO_2 plot; b: Nb/Y vs. Ta/Yb plot; c: Nb vs. Y plot; d: Th vs. Zr/Sr plot. Note the well-defined and distinct groups of each member. e: Spider plot of trace elements of each member. There are significant negative anomalies in case of Nb, Sr, and Ti. Ostoros Member magmatic and Ostoros member phreatomagmatic shows identical run, furthermore Jató Member – Demjén and Jató Member are also identical.

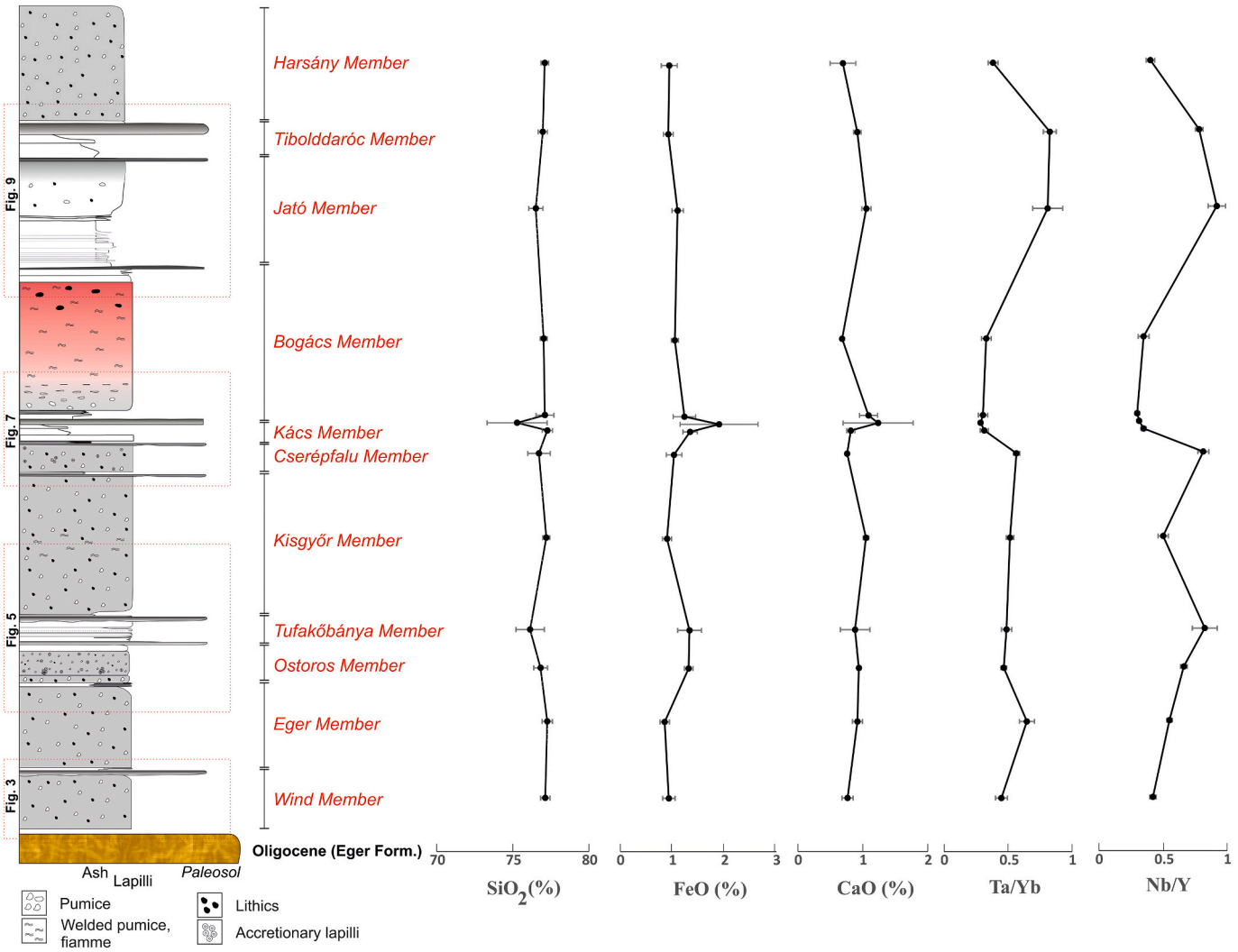

Fig. 12. The complete field-based stratigraphic column of the BFVA. The ignimbrites of the reddish-colored of Bogács Member suggests that ignimbrite is welded (left panel). Next to the member names, the mean geochemical concentrations of major elements and trace element ratios (with standard deviation marked with solid lines) are depicted (right panel). Kács Member contains 3 points, see text for details.

are calc-alkaline, but alkaline samples are also present. The dilute phreatomagmatic PDC deposit of the Tufakőbánya Member shows slightly scattered major and trace element compositions, especially for TiO_2 (Fig. 11a). Groups can be distinguished on the FeO vs. TiO_2 plots, because SiO_2 in Harker diagrams shows very low variability between members. Different outcrops of the Jató Member (Bogács-Tibolddaróc vs. Demjén) show slightly different SiO_2, FeO and TiO_2 contents, which only partly overlap on the discrimination plot. This slight difference of geochemical composition can be also observed in trace elements, e.g., Nb/Y ratio (Fig. 11c). However, we assume that despite this difference, these outcrops represent the same eruption (or at least different phases of the eruption) based on recent zircon U-Pb age (Demjén: 14.94 ± 0.14 Ma vs. Bogács-Tibolddaróc: 14.880 ± 0.014 Ma; Lukács et al., 2018) and the identical phenocryst assemblage (biotite, feldspar, green amphibole; latter is unique in the BFVA), where quartz is absent in contrast to most of the other members of the BFVA.

As seen in Fig. 12 (i.e., major and trace element variations over time), consistent changes in the geochemical compositions during the volcanic evolution of the BFVA cannot be recognized. The element ratios are also changing randomly between members. Since most eruption centers of the members can be poorly constrained (see Biró et al., 2020, 2022; Hencz et al., 2021a; Karátson et al., 2022), classification based on source area is not possible either.

Spider diagrams (Fig. 11e) of the pyroclastic deposits of the BFVA show strong enrichment of some LILEs (large ion lithophile elements, like Cs, Ba, Rb) as well as Pb, U and Th relative to HFSEs (high field strength elements, like Nb, Ta) and light rare earth elements (e.g., La and Ce). Negative anomalies of Sr and to lesser extent Ba and Eu suggest plagioclase (Sr, Eu) and sanidine (Ba, Sr) crystallization. Depletion in Ti suggest titanomagnetite and ilmenite crystallization. Samples from both localities of the Jató Member have highly similar trace element distribution and distinctively high Cs content (>600 ppm) than the other pyroclastic deposits. In the case of Harsány Member, the lowest Sr content (ca. 1.5 ppm on average) can be noticed. Weak Zr negative anomaly and sub-chondritic Zr/Hf in all samples suggests zircon crystallization.

5. Discussion

5.1. Eruption event-scale stratigraphy of the BFVA

At least 13 large explosive eruption events occurred during the volcanic evolution of the BFVA, as witnessed by their deposits identified in the field. The most voluminous pyroclastic deposits are rhyolitic ignimbrites, which can reach 300–350 m in total thickness in boreholes drilled in the middle part of the BFVA (Szakács et al., 1998; Lukács et al.,

2010). However, these core samples were recovered from 50 to 60 year-old boreholes, and they are either not available for examination and further analyses or are damaged; even if descriptions and basic documentation are accessible, these do not provide high-resolution information which necessary for an event-scale study.

The thickest ignimbrite is probably that of the Kisgyőr Member (ca. 80–100 m), which shows welded facies at its east occurrences (e.g., Sály – Latorvár) and nonwelded facies in the west (e.g., Eger – Tufakőbánya). Its eruption center can be inferred in the eastern vicinity of the BFVA as its thickness increases eastwards together with the thickness of the basal fallout layer (Hencz et al., 2021a; see also in Fig. 13c). Similar systematic increase of fallout pumice thickness from west to east has been confirmed for the similar-magnitude (VEI $\geq$ 7) ignimbrite of the Eger Member outlining an eruptive vent south of Eger, i.e., southwest of BFVA (Karátson et al., 2022).

Although, Plinian-type eruptions dominated the volcanism producing ignimbrites (some of them, e.g., the above-mentioned ones, are likely caldera-forming), there are also some less voluminous pyroclastic deposits which can be identified. Between the thick and massive ignimbrites, there are several deposits formed from dilute PDCs (e.g., Tu-1 of Tufakőbánya Member) suggesting smaller-scale eruption events in terms of volume and areal distribution. Many members contain deposits of phreatomagmatic silicic eruptions (Walker, 1981; Sheridan and Wohletz, 1983; Morrissey et al., 2000; Németh and Kósik, 2020), which may have been a common process during the volcanism of the BFVA (Szakács et al., 1998; Biró et al., 2020). Related, significant-volume phreatomagmatic ignimbrites (cf. Wilson et al., 2006; Porreca et al., 2008; Trolese et al., 2017) are also present. The presence of 10–70 cm thick fallout deposits and thin dilute PDC deposits suggest and confirm the assumption that BFVA lay in medial to distal position (15–50 km far; Szakács et al., 1998; Lukács et al., 2010; Biró et al., 2020; Hencz et al., 2021a; Karátson et al., 2022) relative to the eruption centers that were presumably located at the southern margin of the BFVA (Fig. 13c).

The frequently observed reworked pyroclastic rocks can be connected to *syn*-eruptive terrestrial erosional and depositional processes, such as mass flows, sheet wash, or remobilization/redeposition by linear

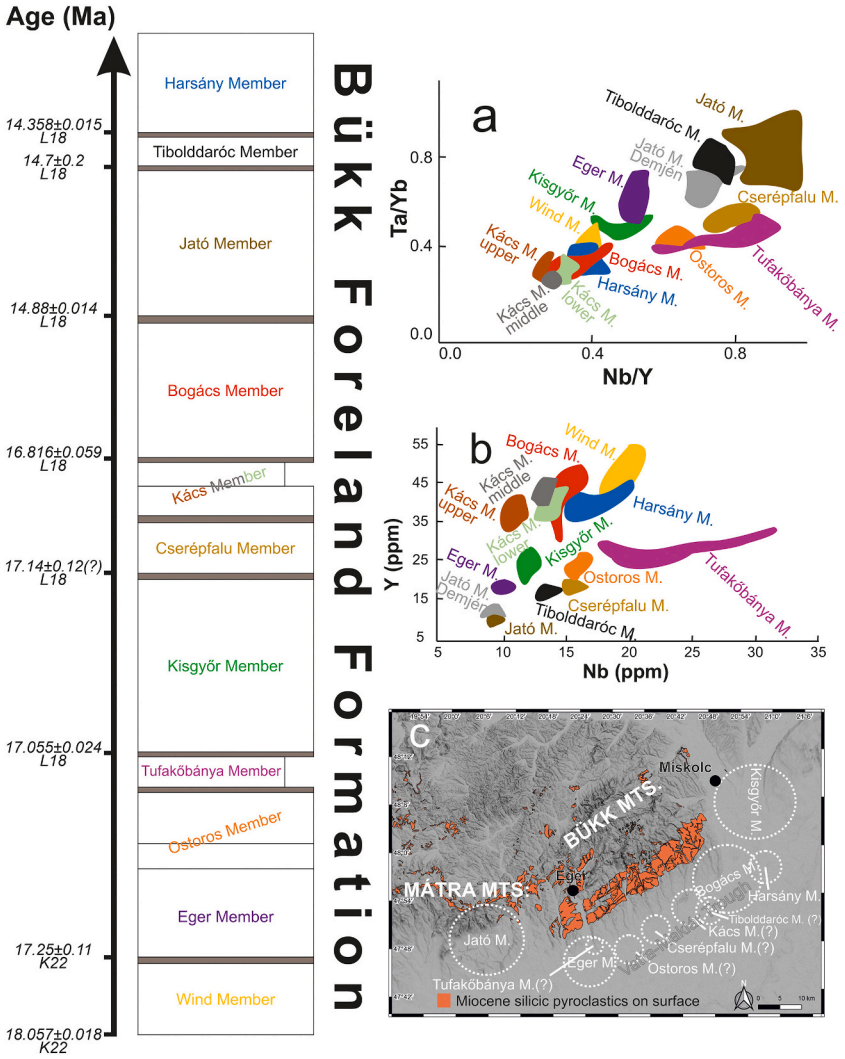

Fig. 13. Concluding figure of the new proposed stratigraphic systematics of the BFVA using all available age data (L18: Lukács et al., 2018; K22: Karátson et al., 2022). In the lithostratigraphic column (left panel) thick brown lines represent the second-order unconformities (paleosols), separating the members. a and b: the most relevant geochemical plots (Nb/Y vs. Ta/Yb and Nb vs. Y) used for member discrimination. c: inferred eruption centers (mostly located in the Vatta-Maklár Trough) for each member based on the spatial distribution of their pyroclastics. '?' symbolizes the members with a highly questionable position for the eruption center. Location of the eruption center of Kisgyőr Member was inferred by Hencz et al. (2021a), Jató Member by Biró et al. (2020), Eger Member by Karátson et al. (2022), and Bogács Member by Szakács et al. (1998) and Biró et al. (2022). Radius of each source-representing circle is proportional with the hypothetical volume of the erupted pyroclastic material based on field observations (e.g., layer thicknesses, spatial distribution). (For interpretation of the references to colour in this figure legend, the reader is referred to the web version of this article.)

fluvial stream flows. In the BFVA, unequivocally underwater-deposited pyroclastics (containing remains of marine fauna or flora) were not identified.

5.2. Correlation using field volcanology and glass geochemistry

Glass major and trace element geochemistry is widely used in volcanic stratigraphy for regional correlation purposes (Lebti et al., 2006; Lowe, 2011; Karátson et al., 2016; Lowe et al., 2017), especially in tephrochronology (e.g., Shane et al., 1998; Wulf et al., 2004, 2016; Albert et al., 2012; Danišik et al., 2021). Although, we do not focus here on regional correlation, it is possible to make some considerations on lithostratigraphic correlation of the field-examined and identified deposits thanks to their geochemical fingerprints, separating pyroclastic units and linking them to different lithofacies.

Similar major and trace element compositions were obtained from glasses sampled from both the Ostoros magmatic and Ostoros phreatomagmatic ignimbrites (Fig. 11). The REE distribution patterns are also strictly similar in both cases (Fig. 11). They also show identical grouping on the discriminant plots (Fig. 11a, b, c, d). As already mentioned, no unconformity (e.g., erosional surface, paleosol) is visible between the magmatic and phreatomagmatic ignimbrites. Merely a 10 cm thick lapilli tuff layer was found interbedded in between, mainly consisting of abundant core-rim type (Van Eaton and Wilson, 2013) accretionary lapilli. The lower and upper contact of this layer is rather transitional than sharp, and there is not any sign of significant time gap between the eruptions. Adding the chemical similarity to the picture, it can be concluded that both ignimbrites of the Ostoros Member were fed by the same magma batch from the same eruption center, deposited possibly during one single eruption event, whereas an abrupt change in eruptive style occurred during the eruption due to changing external factors (i.e., access of external water to the erupting vent). Consequently, the magmatic and phreatomagmatic ignimbrites of this succession can be classified as belonging to the same member (Ostoros Member).

There is some recently published evidence according to which the ignimbrite at Demjén – Nagyeresztvény locality is identical with the ignimbrite of the Jató Member (Biró et al., 2020): very similar zircon U-Pb ages (14.92 ± 0.08 Ma for Td-H unit, i.e., the ignimbrite of the Jató Member, and 14.88 ± 0.014 Ma for Demjén – Nagyeresztvény; Lukács et al., 2015, 2018), zircon and bulk rock trace element geochemistry, zircon textures, and presence of green amphibole in the phenocryst population (Lukács et al., 2015, 2018; Biró et al., 2020). However, regarding trace elements or trace element ratios shown in this paper (e.g., Nb/Y vs. Ta/Yb; Fig. 11b), the rocks exposed at these two sites are not completely overlapping (see Fig. 11b). The physical appearance of the ignimbrite at Demjén – Nagyeresztvény is simple: its thickness is over 20 m, and in the middle part it is welded and contains fiamme. At Bogács cellars, the ignimbrite at the identical stratigraphic position is 5–6 m thick and fine-grained. Because only a small slice of the whole sequence is exposed in Demjén, existence of unconformities cannot be excluded, which may reflect a geochemical 'gradient' in the ignimbrite (i.e., few days- to weeks-long interruption in the volcanism, then resumed activity from a slightly distinct magma batch). The zircon U-Pb dating is not able to resolve such eruption-scale differences (see discussion of zircon U-Pb vs. Ar-Ar dating for other ignimbrites, e.g., Karátson et al., 2022). Hence, although the ignimbrite of the two sites may be handled as erupted from the same eruption center, based on identical phenocrystal assemblage and zircon geochemistry (Lukács et al., 2022), nearly at the same time (Lukács et al. (2018)), the member possibly comprises subsequent flow units with slightly different geochemical compositions. Presumably, more flow units can be separated within this member in the vicinity of the Mátra Mountains, where this member is more widespread ("Tar Dacite Lapilli Tuff Formation": Lukács et al., 2022).

The geochemically studied samples reveal some distinct geochemical features allowing their discrimination (Nb vs. Y, and Nb/Y vs. Ta/Yb; Fig. 13 a, b). The Nb and Y turned out to be useful discriminant elements in the classification (Figs. 12, 13b). In some cases, bimodal distribution of the Nb/Y ratio can be observed (e.g., Harsány Member, Bogács Member). There is a wide range of Nb content in the analyzed glass of the Tufakőbánya. The Ta/Yb and Nb/Y ratios show bimodality and carries the same trace element fingerprint as the underlying Ostoros Member (both the magmatic and phreatomagmatic ignimbrites). Other glass compositions of Tufakőbánya Member differ from any other members of the BFVA. A possible scenario is that a dynamic medium (river, mass flow) picked up the unconsolidated ignimbrite fragments of the Ostoros member and mixed them with the products of a younger pyroclastic flow or fallout material coming from another eruption and deposited the 'mixed' material at the current place.

5.3. Lithostratigraphic scheme of the BFVA - implications on stratigraphic systematics of ancient pyroclastic successions

The BFVA is a mosaic-like, poorly exposed, tectonically fragmented ancient silicic volcanic terrain ca. 400 km^2 large, located today under continental climate, with deeply eroded valleys cut into the unwelded to welded pyroclastics, dense vegetation and soil cover, and showing extensive weathering (Biró et al., 2022). This makes the detailed volcanological reconstruction very difficult.

Proposing and adopting a lithostratigraphic scheme to a volcanic field is always challenging and controversial (see Section 2 and Martí et al., 2018; Németh and Palmer, 2019). In this work, we chose an applicable system of lithostratigraphic systematics of an important volcaniclastic sequence for a relatively small area, which can be later used both for local refinement (in the northern Pannonian basin) and regional correlation. The UBSU scheme of Lucchi (2013) was hybridized with the recommendations of Németh and Palmer (2019). As it can be seen in the detailed stratigraphic columns (Figs. 3, 5, 7, 9), we have built our classification based on the identification of the most relevant lithological features of the layers, i.e., at individual bed (of flow, fall, etc.) level. Then, the lithologies were grouped into 3 types: (1) paleosol, (2) primary volcanic, and (3) reworked. Those primary volcanic deposits not interrupted by unconformity (cf. Lucchi, 2013; similarly to those certainly belonging to the same eruption with typical characteristics of a Plinian eruption sequence, McPhie et al., 1993; Branney and Kokelaar, 2002), were grouped into one lithostratigraphic unit. Similarly, reworked volcaniclastics without UBSU and/or deposited via identical conditions were also classified as a single unit. After this grouping, all units that are not separated by paleosol have been assigned to a member (Fig. 13). Thus, a pyroclastic succession is enrolled into the same member together with its reworked, overlying counterpart, and, therefore, the presence of paleosols plays a critical role in our classification scheme. In the case when no paleosol was formed between two units (e.g., between Eger Member and Ostoros Member), the geochemical differences in the volcanic glass were used to place them in different members. Finally, all members were classified into one single lithostratigraphic formation: the Bükk Foreland Formation. Thus, the process of the classification of the pyroclastic succession from the smallest separable entity to the largest one was as follows: lithologies – units – members – formation (Fig. 12). This new classification (Fig. 13) is quite like the one used in the case of the Cassia Formation (Snake River Plain, Yellowstone hotspot, USA; Knott et al., 2016). Geochemical fingerprinting of the members using volcanic glass trace elements was also successful (Fig. 13a, b). The possible location of the eruption centers, estimated from the field distribution of pyroclastics of each member, is shown in Fig. 13c.

Kács Member is an exception of the scheme, where three different units can be found (Kács Member lower – Ka-1, middle – Ka-2, upper – Ka-3) separated by paleosols without continuously visible transitions, and slightly different geochemical fingerprint. However, the areal distribution of this member is very limited (one single outcrop in Kács village). Thus, the 'paleosol-rule' is not considered in this case, and the member-classification was simplified.

Overall, using fifteen well-documented outcrops (some of them are proposed as type locality for the given member), we were able to create an event-scale lithostratigraphic column despite the challenging conditions. The proposed nomenclature allows the member-level discrimination in the glass geochemistry plots, hence glass geochemistry dataset corroborated by field descriptions can be used as a master database for future regional correlations.

5.4. Paleogeographical and paleoenvironmental settings of the BFVA volcanism

Based on the results presented above, the paleogeographic setting of the BFVA and adjacent areas is characterized by a twofold depositional environment: in the pyroclastic succession there are signs to the presence of a sea cover in the close vicinity of the eruption centers often interacting with the volcanism, and there is also evidence of a terrestrial environment at the site of pyroclastic emplacement. Outside the BFVA, to the west (Mátra Volcanic Area; Figs. 1, 2) an analogous sequence to the Jató Member (the "Tar Dacite Tuff Formation" in Di Capua et al., 2021, or the "Tar Dacite Lapilli Tuff Formation" in Lukács et al., 2022) was described as composed of submarine volcanogenic sediments, which were deposited into a shallow sea (Di Capua et al., 2021). However, the BFVA was fully, or, at least, periodically terrestrial, as suggested by eleven paleosol horizons at different levels in the Bükk Foreland Formation and by the lack of interbedded marine sediments. Paleosols occur at various time horizons and can be found above almost every voluminous ignimbrite. There is no sign of underwater deposition in the succession, on the contrary, the presence of common sub-vertical gas segregation pipes is evident, a feature typical of terrestrial deposition of hot pyroclastic material (Cas and Wright, 1991). Previous studies have already shown that signs of phreatomagmatism could be identified in several pyroclastic deposits of the BFVA (Biró et al., 2020 and references therein). The presence of high amount of water vapor in the eruptional column is remarkably common in the interbedded sequences between the thick ignimbrites (Figs. 6c, f; 8b, c; 10c, d). These include the Eger Member, the newly documented Ostoros member (Os-1), the Tufakőbánya Member (Tu-1), the middle unit of the Kács Member (Ka-2), top of the Bogács Member (Bo-2), and the Jató member (Ja-1). Hence, in the case of seven members there is evidence of water-rich eruption columns, which implies the recurring transgressions of the Central Paratethys Sea in the close vicinity, which heavily impacted the eruption style of explosive eruptions in the BFVA.

A comparable, active volcanic area, which is thought to be analogous to the BFVA from a volcanological and paleoenvironmental point of view is the Taupo Volcanic Zone (TVZ) in New Zealand (as suggested by Biró et al., 2020). Phreatomagmatism was recognized and documented in the case of TVZ in early works (Self and Sparks, 1978; Self, 1983; Wilson, 1993, 2001; Van Eaton and Wilson, 2013). These publications highlighted the possible causes of phreatomagmatism, i.e., the origin of the external water, which has been explained by caldera lakes in most cases, based on, among others, the presence of diatomites in the pyroclastic deposits (Van Eaton and Wilson, 2013). A similar process was described on Santorini, Greece, where seawater-induced phreatomagmatism was responsible for producing the phreatomagmatic pyroclastics of the Minoan Tuff, namely seawater could enter the erupting vent through the collapsed caldera wall during the eruption (Bond and Sparks, 1976; Friedrich and Eriksen, 1988). In the case of the 1906 eruption of Vesuvius, shifting of the eruption style from magmatic-dominant to phreatomagmatic-dominant fragmentation was induced by the tapping of the hydrothermal system (Bertagnini et al., 1991).

In the case of the BFVA, the phreatomagmatic eruption mechanisms, recurring from time to time, can be well explained by the paleoenvironmental setting of the area. During the Early to Middle Miocene, the broader area to which the BFVA belongs was an intensively sinking back-arc basin (Balázs et al., 2016). Subsidence caused multiple transgressions in the Central Paratethys, resulting in intermittent, long-term sea cover in the Carpathian-Pannonian region (Kováč et al., 2017). The subsiding area was occupied by a sea bay, considered to have been an inland sea of the Carpathian-Pannonian region in continuous connection with the wider Paratethys and the ocean (Kováč et al., 2007). Hence, the impact of seawater on volcanism may have been a regional feature: large amounts of surface water were continuously available in the form of seawater at, or in the close vicinity of eruption centers, a conclusion also supported by paleogeographic and paleoenvironmental reconstructions for the Middle Miocene (Kováč et al., 2007, 2017).

In more detail, during this period, the areas inside the Carpathian-Pannonian basin were controlled by a transtension-related tectonic stress field oriented in NE – SW direction (Horváth et al., 1986), which led to the formation of several half-graben structures (Balázs et al., 2016). The subsidence of the basin, coeval with a global sea level rise, resulted in a stepwise transgression of the Central Paratethys in the SE – NW direction in three phases: 16.3–16.2 Ma, ~ 14.7 Ma, 13.6–13.4 Ma (Kováč et al., 2007). As a result, the physiographic appearance of the Carpathian-Pannonian region was that of an archipelago surrounded by both shallow and deep seas. Sea coverage of the broader vicinity of the BFVA was proved earlier by Di Capua et al. (2021) based on micro-scale investigation of volcanogenic sediments and limestones around the Mátra Mountains (few tens of kilometers westward from the BFVA). The area of both the Bükk Mountains and BFVA may have been emergent from this marine environment, forming low-topography terrestrial environments near sea-level during the time of the volcanism (Bérczi et al., 1988; Szakács et al., 1998; Kováč et al., 2017). This reconstruction is supported by the large number of paleosols documented in the BFVA stratigraphic column, which could develop only under terrestrial conditions. Based on these considerations, the eruption centers in the eastern, southern, and western vicinity of BFVA (Fig. 13c; located along the Vatta-Maklár Trough, at maximum a few tens of kilometers from the BFVA; Szakács et al., 1998; Lukács et al., 2010; Biró et al., 2020; Hencz et al., 2021a; Karátson et al., 2022) might have been flooded from time to time by water depending on how sea cover was available in the surrounding areas. Thus, the vents could be opened in a shallow-water or in a flat wetland area (Biró et al., 2020). Such a local setting, as well as the general paleoenvironmental situation, allowed a significant amount of water to be available for water-influenced explosive eruptions.

6. Conclusions

This study documents and interprets the pyroclastic succession of the Miocene silicic volcanism of the Bükk Foreland Volcanic Area (BFVA), Northern Hungary. An event-scale lithostratigraphic column was constructed based on detailed field volcanological investigation corroborated with glass major and trace element geochemistry, documenting each exposed sequence and depositional unit, and thus unraveling the complete volcanic succession, at least that which left marks in the geological record on the surface. Analysis of the documented pyroclastic units, reworked pyroclastics, and frequent paleosols suggest that:

1) the BFVA comprises a narrow strip of medial to distal occurrences of primary and reworked pyroclastic material relative to the source vents inferred to be located south-southeast of the study area, currently subsided in the Pannonian basin, and.
2) a paleoenvironment with at least partial sea cover at eruption centers and, at the same time, a terrestrial emplacement of the volcanic products and subaerial landscape evolution occurred in the area of present-day BFVA. The widespread, long-lasting proximity of sea water induced silicic phreatomagmatism (sensu lato) frequently besides the most voluminous, ignimbrite-forming "dry" magmatic eruptions.

Another major outcome of this study is the presentation of an example of how to undertake a lithostratigraphy-based classification in poorly exposed, deeply eroded, ancient volcanic terrains, highlighting

the importance of field-based investigation in constraining first-order geological framework, thereby creating the basis for more detailed studies. In combination with analysis of volcanic glass geochemistry our approach proved to be very effective in discriminating between volcanic eruption events, even under the strongly weathered conditions of current BFVA.

The compilation of a detailed volcanological description reinforced by glass geochemistry is available as a database in Supplementary Material 4 (Tables S1-S5). The dataset can be used for correlational purposes for Miocene tephras inside and around the Pannonian basin, as well as in the broader areas of Central Europe and the wider Mediterranean region.

CRediT authorship contribution statement

Mátyás Hencz: Conceptualization, Methodology, Investigation, Writing – original draft. **Tamás Biró:** Conceptualization, Methodology, Investigation, Writing – review & editing. **Károly Németh:** Conceptualization, Supervision, Writing – review & editing. **Alexandru Szakács:** Conceptualization, Writing – review & editing. **Maxim Portnyagin:** Methodology, Writing – review & editing, Resources. **Zoltán Cseri:** Investigation. **Zoltán Pécskay:** Writing – review & editing. **Csaba Szabó:** Methodology, Supervision, Writing – review & editing. **Samuel Müller:** Methodology, Resources. **Dávid Karátson:** Conceptualization, Writing – review & editing, Funding acquisition.

Declaration of Competing Interest

The authors declare no competing interests.

Data availability

Geochemical data acquired in this study are provided in Supplementary materials.

Acknowledgements

Work of MH and TB was supported by the ÚNKP-21-4 New National Excellence Program of the Ministry for Innovation and Technology from the source of the Hungarian National Research, Development, and Innovation Fund (ÚNKP-21-4-II-ELTE-382; ÚNKP-21-4-I-ELTE-63). MP and SM thank support from DFG project GA1960/14-1. The research was financed by the Hungarian National Fund (NKFIH-OTKA K131894) and was supported further by a Lendület Research Grant to the MTA-EPSS FluidsByDepth Lendület Research Group (LP-2022-2/2022) provided by the Hungarian Academy of Science. The authors thank Shane Cronin for editorial support and two anonymous reviewers for their suggestions!

Appendix A. Supplementary data

Supplementary data to this article can be found online at https://doi.org/10.1016/j.jvolgeores.2023.107960.

References

Albert, P.G., Tomlinson, E.L., Smith, V.C., Di Roberto, A., Todman, A., Rosi, M., Marani, M., Muller, W., Menzies, M.A., 2012. Marine-continental tephra correlations: Volcanic glass geochemistry from the Marsili Basin and the Aeolian Islands, Southern Tyrrhenian Sea, Italy. J. Volcanol. Geotherm. Res. 229-230, 74–94.

Báez, W., de Silva, S., Chiodi, A., Bustos, E., Giordano, G., Arnosio, M., Suzaño, N., Viramonte, J.G., Norini, G., Groppelli, G., 2020. Pulsating flow dynamics of sustained, forced pyroclastic density currents: insights from a facies analysis of the Campo de la Piedra Pómez ignimbrite, southern Puna, Argentina. Bull. Volcanol. 82, 53. https://doi.org/10.1007/s00445-020-01385-5.

Balázs, A., Matenco, L., Magyar, I., Horváth, F., Cloething, S.A.P.L., 2016. The link between tectonics and sedimentation in back-arc basins: New genetic constraints from the analysis of the Pannonian Basin. Tectonics 35, 1526–1559.

Bérczi, I., Hámor, G., Jámbor, Á., Szentgyörgyi, K., 1988. Neogene sedimentation in Hungary. In: Royden, L.H., Horváth, F. (Eds.), The Pannonian Basin – A Study in Basin Evolution, vol. 45. AAPG Memoir, pp. 57–67.

Bertagnini, A., Landi, P., Santagroce, R., Sbrana, A., 1991. The 1906 eruption of Vesuvius: from magmatic to phreatomagmatic activity through the flashing of a shallow depth hydrothermal system. Bull. Volcanol. 53, 517–532.

Best, M.G., Barr, D.L., Christiansen, E.H., Gromme, S., Deino, A.L., Tingey, D.G., 2009. The Great Basin Altiplano during the middle Cenozoic ignimbrite flareup: insights from volcanic rocks. Int. Geol. Rev. 51 (7–8), 589–633.

Biró, T., Kovács, I.J., Karátson, D., Stalder, R., Király, E., Falus, Gy, Fancsik, T., Sándorné, K.J., 2017. Evidence for post-depositional diffusional loss of hydrogen in quartz phenocryst fragments within ignimbrites. Am. Mineral. 102, 1187–1201.

Biró, T., Hencz, M., Németh, K., Karátson, D., Márton, E., Szakács, A., Bradák, B., Szalai, Z., Pécskay, Z., Kovács, I.J., 2020. A Miocene Phreatoplinian eruption in the North-Eastern Pannonian Basin, Hungary: the Jató Member. J. Volcanol. Geotherm. Res. 401, 106973.

Biró, T., Hencz, M., Telbisz, T., Cseri, Z., Karátson, D., 2022. The relationship between ignimbrite lithofacies and topography in a foothill setting formed on Miocene pyroclastics – a case study from the Bükkalja, Northern Hungary. Hungarian Geogr. Bull. 71, 213–229.

Bond, A., Sparks, R.S.J., 1976. The Minoan eruption of Santorini, Greece. J. Geol. Soc. 132, 1–16.

Branney, M.J., Kokelaar, B.P., 2002. Pyroclastic density currents and the sedimentation of ignimbrites. Geol. Soc. Lond. Mem. 27, 143 p.

Brlek, M., Tapster, S.R., Schindlbeck-Belo, J., Gaynor, S.P., Kutterolf, S., Hauff, F., Georgiev, S.V., Trinajstić, N., Šuica, S., Brčić, V., Wang, K.-L., Lee, Y.-H., Beier, C., Abersteiner, A.B., Mišur, I., Peytcheva, I., Kukoč, D., Németh, B., Trajanova, M., Balen, D., Guillong, M., Szymanowski, D., Lukács, R., 2023. Tracing widespread Early Miocene ignimbrite eruptions and petrogenesis at the onset of the Carpathian-Pannonian Region silicic volcanism. Gondwana Res. 113, 40–60.

Capaccioni, B., Coradossi, N., Harangi, R., Harangi, Sz, Karátson, D., Sarocchi, D., Valentini, L., 1995. Early Miocene pyroclastic rocks of the Bükkalja Ignimbrite Field (North Hungary) – a preliminary stratigraphic report. Acta Vulcanol. 7, 119–124.

Cas, R.A.F., Wright, J.V., 1991. Subaqueous pyroclastic flows and ignimbrites: an assessment. Bull. Volcanol. 53, 357–380.

Csontos, L., Nagymarosy, A., Horváth, F., 1992. Tertiary evolution of the Intra-Carpathian area: a model. Tectonophysics 208, 221–241.

Czuppon, Gy, Lukács, R., Harangi, Sz, Mason, P.R.D., Ntaflos, T., 2012. Mixing of crystal mushes and melts in the genesis of the Bogács ignimbrite suite, northern Hungary: an integrated geochemical investigation of mineral phases and glasses. Lithos 148, 71–85.

Danišik, M., Ponomareva, V., Portnyagin, M., Popov, S., Zastrozhnov, A., Kirkland, C.L., Evans, N.J., Konstantinov, E., Hauff, F., Garbe-Schönberg, D., 2021. Gigantic eruption of a Carpathian volcano marks the largest Miocene transgression of Eastern Paratethys. Earth Planet. Sci. Lett. 563, 116890.

Di Capua, A., Scasso, R.A., 2020. Sedimentological and petrographic evolution of a fluvio-lacustrine environment during the onset of volcanism: Volcanically-induced forcing of sedimentation and environmental responses. Sedimentology 67 (4), 1879–1913.

Di Capua, A., Barilaro, F., Szepesi, J., Lukács, R., Gál, P., Norini, G., Sulpizio, R., Soós, I., Harangi, S., Groppelli, G., 2021. Correlating volcanic dynamics and the construction of a submarine volcanogenic apron: an example from the Badenian (Middle Miocene) of North-Eastern Hungary. Mar. Pet. Geol. 126, 104944.

Friedrich, W.L., Eriksen, U., 1988. Existence of a Water-Filled Caldera prior to the Minoan Eruption of Santorini, Greece. Naturwissenschaften 75, 567–569.

Gyalog, L., Budai, T., 2004. Proposal for new lithosratigraphic units of Hungary, 2002. Annual report of the Geological Institute of Hungary, pp. 195–232 (in Hungarian with English abstract).

Harangi, Sz, Mason, P.R.D., Lukács, R., 2005. Correlation and petrogenesis of silicic pyroclastic rocks in the Northern Pannonian Basin, Eastert-Central Europe: in situ trace element data of glass shards and mineral chemical contstraints. J. Volcanol. Geotherm. Res. 143, 237–257.

Hencz, M., Biró, T., Cseri, Z., Karátson, D., Márton, E., Németh, K., Szakács, A., Pécskay, Z., Kovács, I.J., 2021a. A lower Miocene pyroclastic-fall deposit from the Bükk Foreland Volcanic Area, Northern Hungary: Clues for an eastward-located source. Geol. Carpath. 72 (1), 26–47.

Hencz, M., Biró, T., Cseri, Z., Németh, K., Szakács, A., Márton, E., Pécskay, Z., Karátson, D., 2021b. Signs of complex eruption events at the Bükk Foreland (Northern-Hungary): the Kács Member. In: 22nd Mining, Metallurgy and Geology Conference 2021. Hungarian Technical Scientific Society of Transylvania, pp. 71–75. Abstract Book. (in Hungarian with English abstract).

Hencz, M., Biró, T., Kovács, I.J., Stalder, R., Németh, K., Szakács, A., Pálos, Zs, Pécskay, Z., Karátson, D., 2021c. Uniform "water" content in quartz phenocrysts from silicic pyroclastic fallout deposits – implications on pre-eruptive conditions. Eur. J. Mineral. 33, 571–589.

Horváth, F., Dövényi, P., Laczó, I., 1986. Geothermal effect of magmatism and its contribution to maturation of the organic matter in sedimentary basins. In: Buntebarth, G., Stegena, L. (Eds.), Paleogeothermics, Lecture Notes in Earth Sci, vol. 5. Springer-Verlag, Berlin, Heidelberg, pp. 173–183.

Karátson, D., Wulf, S., Veres, D., Magyari, E.K., Gertisser, R., Timar-Gabor, A., Novothny, Á., Telbisz, T., Szalai, Z., Anechitei-Deacu, V., Appelt, O., Bormann, M., Jánosi, Cs, Hubay, K., Schäbitz, F., 2016. The latest explosive eruptions of Ciomadul (Csomád) volcano, East Carpathians – a tephrostratigraphic approach for the 51-29 ka BP time interval. J. Volcanol. Geotherm. Res. 319, 29–51.

Karátson, D., Biró, T., Portnyagin, M., Kiss, B., Paquette, J.-L., Cseri, Z., Hencz, M., Németh, K., Lahitte, P., Márton, E., Kordos, L., Józsa, S., Hably, L., Müller, S.,

Szarvas, I., 2022. Large-magnitude (VEI ≥ 7) 'wet' explosive silicic eruption preserved a lower Miocene habitat at the Ipolytarnóc Fossil Site, North Hungary. Sci. Rep. 12, 9743.
Knott, T.R., Branney, M.J., Reichow, M.K., Finn, D.R., Coe, R.S., Storey, M., Barfod, D., McCurry, M., 2016. Mid-Miocene record of large-scale Snake River-type explosive volcanism and associated subsidence on the Yellowstone hotspot track: the Cassia Formation of Idaho, USA. GSA Bull. 128 (7–8), 1121–1146.
Kováč, M., Andreyeva-Grigorovich, A., Bajraktarevic, Z., Brzobohatý, R., Filipescu, S., Fodor, L., Harzhauser, M., Nagymarosy, A., Oszczypko, N., Pavelic, D., 2007. Badenian evolution of the Central Paratethys Sea: paleogeography, climate and eustatic sea-level changes. Geol. Carpath. 58, 579–606.
Kováč, M., Hudáčková, N., Halásova, E., Kováčová, M., Holcová, K., Oszczypko-Clowes, M., Báldi, K., Less, G., Nagymarosy, A., Ruman, A., Klučiar, T., 2017. The Central-Paratethys paleoceanography: a water circulation model based on microfossil proxies, climate, and changes of depositional environment. Acta Geol. Slovaca 9, 75–114.
Kovács, I., Szabó, Cs, 2008. Middle Miocene volcanism in the vicinity of the Middle Hungarian zone: evidence for an inherited enriched mantle source. J. Geodyn. 45, 1–15.
Lavigne, F., Thouret, J.C., Voight, B., Suwa, H., Sumaryno, A., 2000. Lahars at Merapi volcano, Central Java: an overview. J. Volcanol. Geotherm. Res. 100, 423–456.
Lebti, P.P., Thouret, J.-C., Wörner, G., Fornari, M., 2006. Neogene and Quaternary ignimbrites in the area of Arequipa, Southern Peru: Stratigraphical and petrological correlations. J. Volcanol. Geotherm. Res. 154, 251–275.
Lowe, D.J., 2011. Tephrochronology and its application: a review. Quat. Geochronol. 6 (2), 107–153.
Lowe, D.J., Pearce, N.J.G., Jorgensen, M.A., Kuehn, S.C., Tryon, C.A., Hayward, C.L., 2017. Correlating tephras and cryptotephras using glass compositional analyses and numerical and statistical methods: Review and evaluation. Quat. Sci. Rev. 175, 1–44.
Lucchi, F., 2013. Stratigraphic methodology for the geological mapping of volcanic areas; insights from the Aeolian Archipelago (southern Italy). Geol. Soc. Lond. Mem. 37, 37–53.
Lukács, R., Harangi, Sz, Ntaflos, T., Mason, P.R.D., 2005. Silicate melt inclusions in the phenocrysts of the Szomolya Ignimbrite, Bükkalja Volcanic Field (Northern Hungary): Implications for magma chamber processes. Chem. Geol. 223, 46–67.
Lukács, R., Harangi, Sz, Mason, P.R.D., Ntaflos, T., 2009. Bimodal pumice populations in the 13.5 Ma Harsány ignimbrite, Bükkalja Volcanic Field, Northern Hungary: Syn-eruptive mingling of distinct rhyolitic magma batches? Centr. Eur. Geol. 52, 51–72.
Lukács, R., Harangi, Sz, Radóc, Gy, Kádár, M., Pécskay, Z., Ntaflos, T., 2010. The Miocene pyroclastic rocks of the boreholes Miskolc–7, Miskolc–8 and Nyékládháza–1 and their correlation with the ignimbrites of Bükkalja. Földtani Közlöny 140, 31–48 (in Hungarian with English abstract).
Lukács, R., Harangi, Sz, Bachmann, O., Guillong, M., Danisik, M., Buret, Y., von Quadt, A., Dunkl, I., Fodor, L., Sliwinski, J., Soós, I., Szepesi, J., 2015. Zircon geochronology and geochemistry to constrain the youngest eruption events and magma evolution of the Mid-Miocene ignimbrite flare-up in the Pannonian Basin, eastern-Central Europe. Contrib. Mineral. Petrol. 170, 1–26.
Lukács, R., Harangi, Sz, Guillong, M., Bachmann, O., Fodor, L., Buret, Y., Dunkl, I., Sliwinski, J., von Quadt, A., Peytcheva, I., Zimmerer, M., 2018. Early to Mid-Miocene syn-extensional massive silicic volcanism in the Pannonian Basin (East-Central Europe): Eruption chronology, correlation potential and geodynamic implications. Earth Sci. Rev. 179, 1–19.
Lukács, R., Guillong, M., Bachmann, O., Fodor, L., Harangi, Sz, 2021. Tephrostratigraphy and Magma Evolution based on combined Zircon Trace Element and U-Pb Age Data: Fingerprinting Miocene Silicic Pyroclastic Rocks in the Pannonian Basin. Front. Earth Sci. 9, 615768 https://doi.org/10.3389/feart.2021.615768.
Lukács, R., Harangi, Sz, Gál, P., Szepesi, J., Di Capua, A., Norini, G., Sulpizio, R., Groppelli, G., Fodor, L., 2022. Formal definition and description of lithostratigraphic units related to the Miocene silicic pyroclastic rocks outcropping in Northern Hungary: a revision. Geol. Carpath. 73 (2), 137–158.
Martí, J., Groppelli, G., Brum da Silveira, A., 2018. Volcanic stratigraphy: a review. J. Volcanol. Geotherm. Res. 357, 68–91.
Márton, E., Pécskay, Z., 1998. Complex evaluation of paleomagnetic and K/Ar isotope data of the Miocene ignimbritic volcanics in the Bükk Foreland, Hungary. Acta Geol. Hung. 41, 467–476.
McPhie, J., Doyle, M., Allen, R., 1993. Volcanic Textures – A Guide to the Interpretation of Textures in Volcanic Rocks. University of Tasmania, Centre for Ore Deposit and Exploration Studies, Hobart, Tasmania. ISBN 0 85901 522 X, 196 p.
Morrissey, M.M., Zimanowski, B., Wohletz, K., Buettner, R., 2000. Phreatomagmatic fragmentation. In: Sigurdsson, H., Houghton, B., McNutt, S., Rymer, H., Stix, J. (Eds.), The Encyclopedia of Volcanoes, First edition. Academic Press, San Diego, USA, pp. 431–445.
Németh, K., Kósik, Sz, 2020. Review of explosive hydrovolcanism. Geosciences 10, 44. https://doi.org/10.3390/geosciences10020044.
Németh, K., Palmer, J., 2019. Geological mapping of volcanic terrains: Discussion on concepts, facies models, scales, and resolutions from New Zealand perspective. J. Volcanol. Geotherm. Res. 385, 27–45.
Pécskay, Z., Lexa, J., Szakács, A., Seghedi, I., Balogh, K., Konečný, V., Zelenka, T., Kovács, M., Póka, T., Fülöp, A., Márton, E., Panaiotu, C., Cvetković, V., 2006. Geochronology of Neogene magmatism in the Carpathian arc and intra-Carpathian area. Geol. Carpath. 57, 511–530.
Póka, T., Zelenka, T., Szakács, A., Seghedi, I., Nagy, G., Simonits, A., 1998. Petrology and geochemistry of the Miocene acidic explosive volcanism of the Bükk Foreland; Pannonian Basin, Hungary. Acta Geol. Hung. 41, 399–428.
Porreca, M., Mattei, M., MacNiocaill, C., Giordano, G., McClelland, E., Funiciello, R., 2008. Paleomagnetic evidence for low-temperature emplacement of the phreatomagmatic Peperino Albano ignimbrite (Colli Albani volcano, Central Italy). Bull. Volcanol. 70, 877–893.
Rybár, S., Šarinová, K., Sant, K., Kuiper, K.F., Kováčová, M., Vojtko, R., Reiser, M.K., Fordinál, K., Teodoridis, V., Nováková, P., Vlček, T., 2019. New $^{40}Ar/^{39}Ar$, fission track and sedimentological data on a middle Miocene tuff occurring in the Vienna Basin: Implications for the north-western Central Paratethys region. Geol. Carpath. 70, 386–404.
Seghedi, I., Downes, H., Szakács, A., Mason, P.R.D., Thirwall, M.F., Rosu, E., Pécskay, Z., Márton, E., Panaiotu, C., 2004. Neogene-Quaternary magmatism and geodynamics in the Carpathian-Pannonian region: a synthesis. Lithos 72, 117–146.
Seghedi, I., Downes, H., Harangi, Sz, Mason, P.R.D., Pécskay, Z., 2005. Geochemical response of magmas to Neogene-Quaternary continental collision in the Carpathian-Pannonian region: a review. Tectonophysics 410, 485–499.
Segschneider, B., Landis, C.A., Manville, V., White, J.D.L., Wilson, C.J.N., 2002. Environmental response to a large, explosive rhyolite eruption: Lithofacies and physical sedimentology of post-1.8 ka pumice-rich Taupo volcaniclastics in the Hawke Bay region, New Zealand. Sediment. Geol. 150, 275–299.
Self, S., 1983. Large-scale phreatomagmatic silicic volcanism: a case study from New Zealand. J. Volcanol. Geotherm. Res. 17, 433–469.
Self, S., Sparks, R.S.J., 1978. Characteristics of Widespread Pyroclastic Deposits formed by the Interaction of Silicic Magma and Water. Bull. Volcanol. 41, 196–212.
Shane, P., Black, T., Eggins, S., Westgate, J., 1998. Late Miocene marine tephra beds: Recorders of rhyolitic volcanism in North Island, New Zealand. New Zeal. J. Geol. Geophys. 41 (2), 165–178.
Sheridan, M.F., Wohletz, K.H., 1983. Hydrovolcanism: basic considerations and review. J. Volcanol. Geotherm. Res. 17, 1–29.
Solleiro-Rebolledo, E., Sedov, S., Gama-Castro, J., Flores-Román, D., Ecamilla-Sarabia, G., 2003. Paleosol-sedimentary sequences of the Glacis de Buenavista, Central Mexico: interaction of Late Quaternary pedogenesis and volcanic sedimentation. Quat. Int. 106–107, 185–201.
Szabó, Cs, Harangi, Sz, Csontos, L., 1992. Review of Neogene and Quaternary volcanism of the Carpathian-Pannonian Region. Tectonophysics 208, 243–256.
Szakács, A., Márton, E., Póka, T., Zelenka, T., Pécskay, Z., Seghedi, I., 1998. Miocene acidic explosive volcanism in the Bükk Foreland, Hungary: identifying eruptive sequences and searching for source locations. Acta Geol. Hung. 41, 413–435.
Szakács, A., Pécskay, Z., Gál, Á., 2018. Patterns and trends of time–space evolution of Neogene volcanism in the Carpathian–Pannonian region: a review. Acta Geodaetica Geophys. 53, 347–367.
Trolese, M., Giordano, G., Cifelli, F., Winkler, A., Mattei, M., 2017. Forced transport of thermal energy in magmatic and phreatomagmatic large volume ignimbrites: Paleomagnetic evidence from the Colli Albani volcano, Italy. Earth Planet. Sci. Lett. 478, 179–191.
Van Eaton, A.R., Wilson, C.J.N., 2013. The nature, origins and distribution of ash aggregates in a large-scale wet eruption deposit: Oruanui, New Zealand. J. Volcanol. Geotherm. Res. 250, 129–154.
Walker, G.P.L., 1981. Characteristics of two phreatoplinian ashes, and their water-flushed origin. J. Volcanol. Geotherm. Res. 9, 395–407.
White, J.D.L., Valentine, G.A., 2016. Magmatic versus phreatomagmatic fragmentation: Absence of evidence is not evidence of absence. Geosphere 12 (5), 1478–1488.
Wilson, C.J.N., 1993. Stratigraphy, chronology, styles and dynamics of late Quaternary eruptions from Taupo volcano, New Zealand. Phil. Trans. Phys. Sci. Eng. 343, 205–306.
Wilson, C.J.N., 2001. The 26.5 ka Oruanui eruption, New Zealand: an introduction and overview. J. Volcanol. Geotherm. Res. 112, 133–174.
Wilson, C.J.N., Blake, S., Charlier, B.L.A., Sutton, A.N., 2006. The 26.5 ka Oruanui eruption, Taupo volcano, New Zealand: development, characteristics and evacuation of a large rhyolitic magma body. J. Petrol. 47, 35–69.
Wulf, S., Kraml, M., Brauer, A., Keller, J., Negendank, J.F.W., 2004. Tephrochronology of the 100 ka lacustrine sediment record of Lago Grande di Monticchio (southern Italy). Quat. Int. 122, 7–30.
Wulf, S., Fedorowicz, S., Veres, D., Lanczont, M., Karátson, D., Gertisser, R., Bormann, M., Magyari, E., Appelt, O., Hambach, U., Gozhyk, P.F., 2016. The 'Roxolany Tephra' (Ukraine) – new evidence for an origin from Ciomadul volcano, East Carpathians. J. Quat. Sci. 31 (6), 565–576.